European Journal of Pharmacology 862 (2019) 172623

Contents lists available at ScienceDirect

European Journal of Pharmacology

journal homepage: www.elsevier.com/locate/ejphar

Full length article

# Combined treatment with SB203580 and dexamethasone suppresses non-typeable *Haemophilus influenzae*-induced Th17 inflammation response in murine allergic asthma

Guoqiang Wang[a], Zhiqiang Pang[a], Alan Chen-Yu Hsu[b], Xuewa Guan[a], Nan Ran[a], Yuze Yuan[a], Ziyan Wang[a], Yingqiao Guo[c], Ruipeng Zheng[a,d], Fang Wang[a,*]

[a] Department of Pathogen Biology, College of Basic Medical Sciences, Jilin University, Changchun, 130021, China
[b] Priority Research Centre for Asthma and Respiratory Diseases, Hunter Medical Research Institute and the University of Newcastle, NSW, 2305, Australia
[c] Department of Genetics, College of Basic Medical Sciences, Jilin University, Changchun, 130021, China
[d] Department of Invasive Technology, First Hospital of Jilin University, Changchun, 130021, China

ARTICLE INFO

*Keywords:*
Steroid-resistant asthma
Airway hyper-responsiveness
Non-typeable *Haemophilus influenzae*
Th17 inflammation response
p38 MAPK
SB203580

ABSTRACT

Accumulating evidence suggests that non-typeable *Haemophilus influenzae* (NTHi) infection drives the development of steroid-resistant allergic airway disease (SRAAD), exacerbates clinical symptoms, worsens quality of life, and accounts for most of the related healthcare burden. The poor understanding of the pathogenesis of SRAAD deters the development of more effective therapeutic strategies. Here, we established a murine model of NTHi infection-induced exacerbation of allergic airway disease. We showed that NTHi infection drove Th 17-mediated pulmonary neutrophilic inflammation, aggravated airway hyper-responsiveness, and upset the balance of MUC5AC and MUC5B expression. Dexamethasone treatment effectively inhibited the features of allergic airway disease but failed to reduce NTHi-induced exacerbation, which was associated with the hyper-phosphorylation of p38 mitogen-activated protein kinase (MAPK). Interestingly, inhibition of p38 using a specific inhibitor (SB203580) only partly suppressed the airway hyper-responsiveness and mucus hyper-secretion but failed to abrogate the infection-induced neutrophilic inflammatory response in SRAAD. However, SB203580 and dexamethasone co-treatment substantially suppressed all the features of NTHi-induced SRAAD. Our findings highlight the importance of p38 MAPK in the pathogenesis of NTHi-induced steroid resistance, and this combined treatment approach may be a novel strategy against steroid-resistant asthma.

## 1. Introduction

Asthma is an increasingly prevalent global health problem, affecting over 300 million people worldwide (Reddel et al., 2015). As a heterogeneous airway inflammatory disease, asthma is categorised into different phenotypes, including eosinophilic and neutrophilic asthma (Wang et al., 2011). Th2-driven eosinophilic inflammation, mucus hypersecretion, and airway hyper-responsiveness (AHR) can be controlled by a corticosteroid (Afshar et al., 2013). In contrast, a subpopulation of 5–20% of patients with asthma shows more serious neutrophilic inflammation and a poor response to steroid treatment, defined as steroid-resistant allergic airway disease (SRAAD) (Peters et al., 2019). Patients with this asthma type account for 50–80% of healthcare resources and 30–50% of mortality among patients with asthma (Hansbro et al., 2017). However, the development of more effective strategies is severely hampered by the lack of understanding of the pathogenesis of SRAAD.

Increasing clinical evidence suggests that lower respiratory tract infections caused by *Haemophilus influenza* play pivotal roles in the pathogenesis of steroid-resistant asthma (Moraes and Sears, 2018). For instance, 16S ribosomal-DNA high-throughput sequencing techniques have uncovered higher prevalence of *H. influenzae* among patients with neutrophilic asthma (Marri et al., 2013; Simpson et al., 2016), especially steroid-resistant asthma (76% of cases) (Durack et al., 2017; Goleva et al., 2013). Furthermore, murine studies have shown that non-typeable *Haemophilus influenzae* (NTHi) infection plays a pathogenic role in the development and exacerbation of asthma. Early-life colonisation with NTHi can enhance the secretion of Th2 cytokines, thereby exacerbating such airway diseases in mice (McCann et al., 2016). However, NTHi infection has also been reported to switch Th2-

* Corresponding author.
*E-mail address:* wf@jlu.edu.cn (F. Wang).

https://doi.org/10.1016/j.ejphar.2019.172623
Received 26 April 2019; Received in revised form 14 August 2019; Accepted 20 August 2019
Available online 22 August 2019
0014-2999/ © 2019 Published by Elsevier B.V.

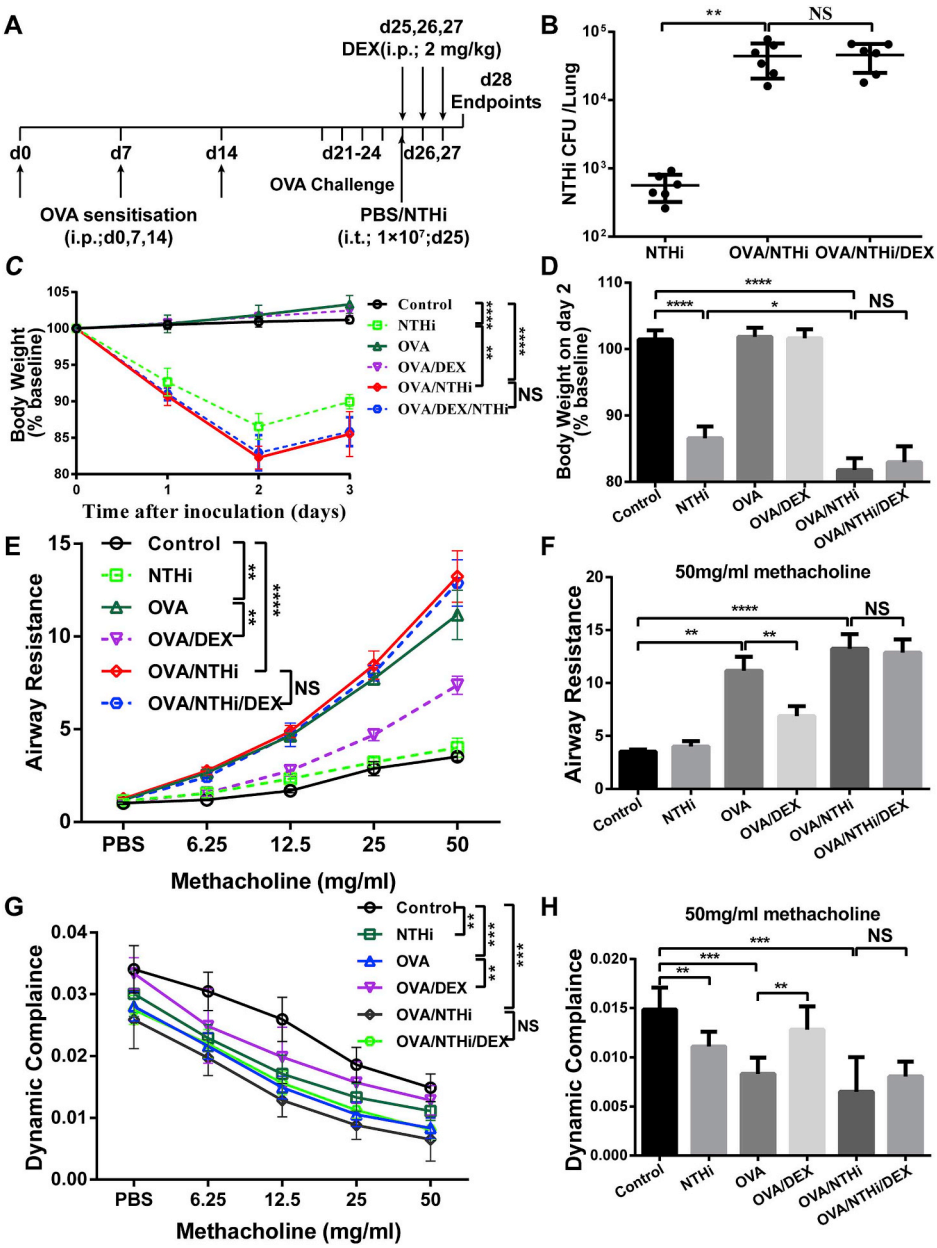


**Fig. 1.** The number of NTHi colonisation in the airways was increased, and lung function was impaired in the OVA/NTHi mice. **(A)** The experimental outline. BALB/c mice were sensitised i.p. with OVA/alum (days 0, 7, and 14) and challenged with the OVA aerosol (days 21–24). The mice were inoculated i.t. with NTHi at $10^7$ CFUs per 30 µl (day 25) to induce SRAAD. Dexamethasone was administered i.p. (days 25–27) to evaluate steroid sensitivity. All the clinical features were quantified on day 28. **(B)** NTHi loads in the lung homogenates were characterised by bacterial colony counting. **(C)** Body weight loss is shown as a percentage of baseline. **(D)** The plot of body weight on day 2 after NTHi infection. AHR was measured as **(E)** Respiratory system resistance in response to increasing concentrations of methacholine, **(F)** Respiratory system resistance in response to 50 mg/ml methacholine, **(G)** dynamic compliance in response to increasing concentrations of methacholine, and **(H)** dynamic compliance in response to 50 mg/ml methacholine. Data are presented as mean ± S.D., n = 6, $^{**}P < 0.01$; $^{***}P < 0.001$; $^{****}P < 0.0001$; NS, non-significant.

mediated eosinophilic inflammation to Th17-driven neutrophilic inflammation (Essilfie et al., 2011). These findings suggest that the timing of NTHi infection may result in different immunopathogenesis of asthma, and the mechanisms underlying the NTHi-induced exacerbation of asthma and the development of steroid resistance remain to be investigated.

The pathogenesis of asthma involves multiple signalling pathways including phosphoinositide-3-kinase (PI3K) (Takeda et al., 2009) and Toll-like receptors (Li et al., 2010). Growing experimental evidence indicates that mitogen-activated protein kinase (MAPK) (Chung, 2011), and the activation of p38, a member of the MAPK family, may induce corticosteroid insensitivity in severe asthma (Bhavsar et al., 2008). Activation of p38 has also been observed in NTHi-induced otitis media and chronic obstructive pulmonary disease (Khalaf et al., 2017; Konduru et al., 2017). Inhibition of p38 activation with the specific pharmacological inhibitor SB203580 has been demonstrated to enhance the anti-inflammatory effects of corticosteroids (Khalaf et al., 2017). However, the mechanisms by which p38 activation drives NTHi-induced asthma exacerbation are yet to be investigated.

In this study, we researched the therapeutic efficacy of SB203580 in a murine model of SRAAD. We first established murine models of NTHi infection and ovalbumin (OVA)-induced allergic airway disease (AAD) and investigated the roles of p38 activation in the pathogenesis and exacerbation of NTHi-induced SRAAD. Next, we demonstrated the potential of the combined treatment with SB203580 and dexamethasone as a novel therapeutic approach to asthma.

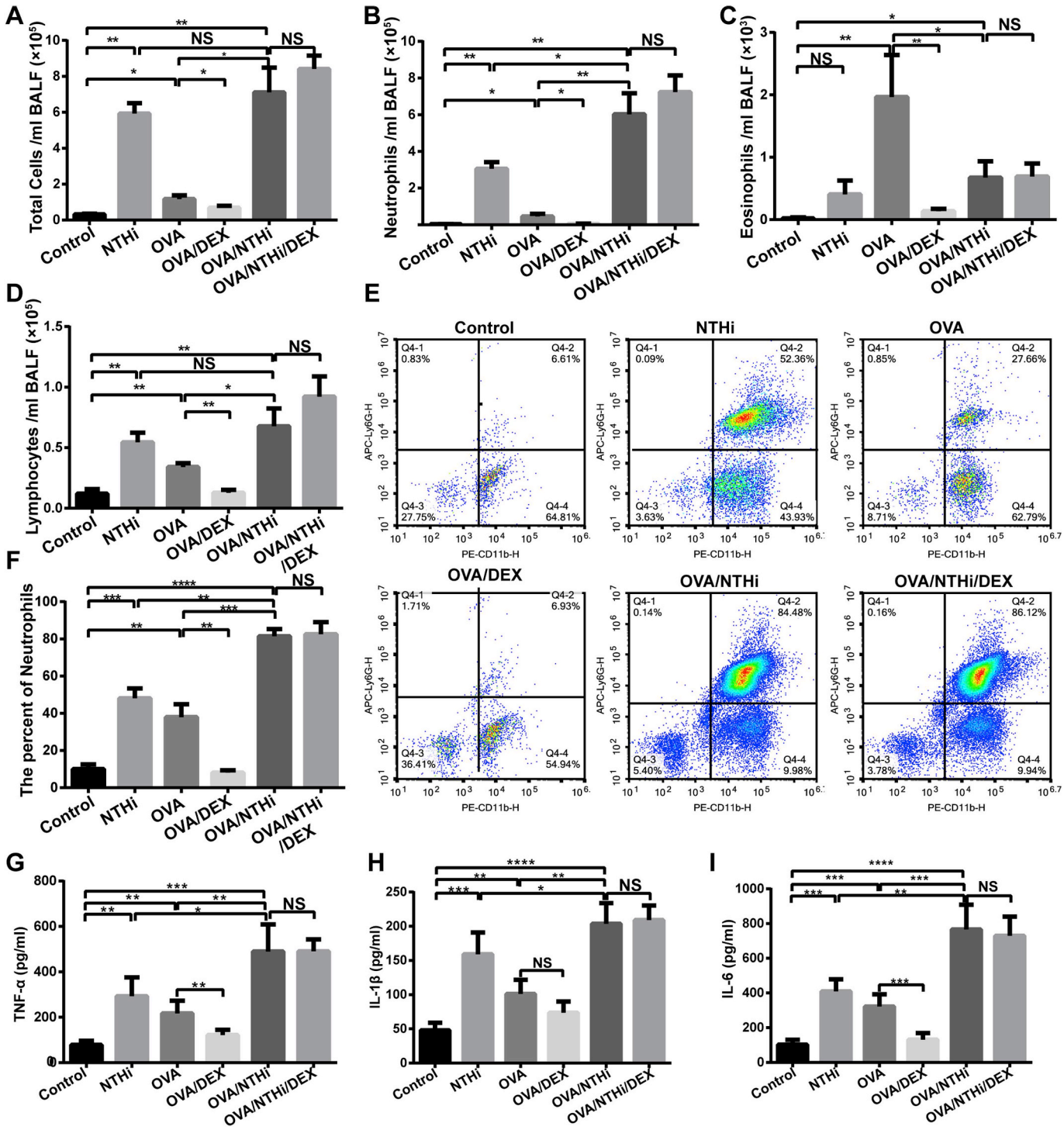


**Fig. 2.** NTHi infection aggravates neutrophilic inflammation in BAL fluid. **(A)** Total cells, **(B)** neutrophils, **(C)** eosinophils, and **(D)** lymphocytes were enumerated in BAL fluid by light microscopy. **(E)** Neutrophils in BAL fluid were detected by flow cytometry, and **(F)** the percentage was analysed. **(G)** TNF-α, **(H)** IL-1β, and **(I)** IL-6 in BAL fluid were quantified by ELISAs. Data are presented as mean ± S.D., n = 6, $^{*}P < 0.05$; $^{**}P < 0.01$; $^{***}P < 0.001$; $^{****}P < 0.0001$; NS, non-significant.

## 2. Materials and methods

### 2.1. Bacterial strains and culture conditions

An NTHi strain (ATCC49247) was prepared as previously described (Guan et al., 2018). Bacteria were cultured on chocolate agar for 18–24 h at 37 °C and 5% $CO_2$, harvested, washed, and diluted with sterile isotonic saline. A diluted concentration, $10^7$ colony-forming units (CFU)/ml, was quantitated at an optical density of 600 nm ($OD_{600}$).

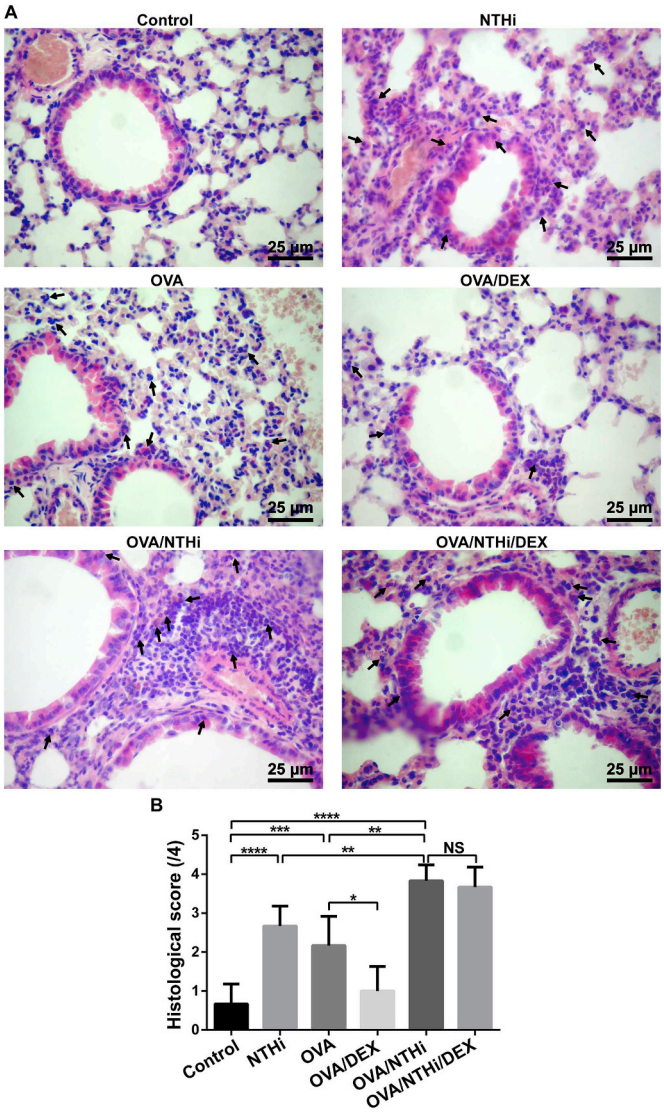


**Fig. 3.** NTHi infection aggravates pulmonary neutrophilic inflammation in AAD. **(A)** Inflammatory infiltrates in lungs were determined by H&E staining (black arrowheads indicate inflammatory cells in the lung). **(B)** The histological score was estimated by H&E staining of lung sections. Data are presented as mean ± S.D., n = 6, $^{*}P < 0.05$; $^{**}P < 0.01$; $^{***}P < 0.001$; $^{****}P < 0.0001$; NS, non-significant.

### 2.2. Experimental protocols

Female BALB/c mice, 6–8 weeks old, were sensitised by intraperitoneal (i.p.) injection with 100 μg of OVA (Grade V, Sigma-Aldrich, St. Louis, MO, USA) mixed with 2 mg of aluminium hydroxide (Thermo Fisher Scientific, Rd. Rockford, IL, USA) in sterile saline (200 μl) on days 0, 7, and 14. They were subsequently challenged with 5% aerosolised OVA for 30 min/day from day 21 to day 24. The mice of the control group were sham-sensitised and challenged with an equivalent volume of saline. The mice were intra-tracheally (i.t.) inoculated either with NTHi ($5 \times 10^5$ CFUs in 30 μl of saline) or with sterile saline under pentobarbital anaesthesia on day 25. Where indicated (Fig. 1A), mice were injected i.p. with dexamethasone (Sigma-Aldrich, Shanghai, China; 2 mg/kg) or the p38 MAPK inhibitor SB203580 (Selleck, Houston, TX, USA; 5 mg/kg) on days 25–27. On day 28, all the mice were anaesthetised and euthanised for the following assays.

### 2.3. Bacterial recovery

The lung tissues of the mice were collected and homogenised with a 9-fold volume of sterile saline on a Tissue Lyser LT tissue disruptor (TissuePrep, Gering, Beijing, China). Serial dilutions of lung homogenates were spread on a chocolate agar plate and cultured for 24 h (37 °C, 5% $CO_2$); then, the colonies were enumerated.

### 2.4. Measurement of AHR

The AHR in response to increasing doses of acetyl-β-methylcholine chloride (Sigma-Aldrich) was assessed by means of a DSI Buxco RC system (Fine Point; St. Paul, MN, USA), as described elsewhere (Hsu et al., 2015; Li et al., 2017). Briefly, mice were anaesthetised with pentobarbital (40 mg/kg) by i.p. injection, and a cannula was inserted into the trachea for ventilation (tidal volume of 8 ml/kg at a rate of 140 breaths/min). The mice were exposed to aerosolised methacholine at a gradually increasing concentration (0, 6.25, 12.5, 25, and 50 mg/ml in saline) for 2 min. Respiratory system resistance and dynamic compliance were calculated in the software provided by DSI Buxco. The results are shown as an average of maximal resistance after each dose of methacholine minus baseline (saline alone) resistance.

### 2.5. Bronchial alveolar lavage (BAL) fluid collection and cell counts

BAL fluid was collected and stained for differential cell counts as previously described (Li et al., 2017). Briefly, a mouse trachea was dissected and attached to a micro syringe, and then, the lung was washed three times with 1 ml of sterile phosphate-buffered saline (PBS). BAL fluid with a recovery rate of more than 85% was centrifuged (300 × *g*, 5 min, 4 °C), and the cell pellets were resuspended in Red Blood Cell Lysis Buffer (Solarbio, Beijing, China). The remaining cells were counted with a haemocytometer and then were cytospun (300 × *g*, 5 min, Ttettich Zentrifugen Universal 320, Australia) onto microscope slides. The slides were dried at room temperature, fixed in 90% ethanol for 10 min, and stained with the Diff Rapid Staining Kit (Solarbio, Beijing, China). Differential leukocyte counts were determined by light microscopy, with the counting of a minimum of 200 cells in each of four random visual fields.

### 2.6. Histopathological and immunohistochemical analyses of lungs

Murine lung lobes were collected, washed, and fixed in 10% buffered formalin for 24 h, and then embedded in paraffin and sectioned (at 5 μm thickness). The tissue sections were stained with haematoxylin & eosin (H&E) to assess histopathological features and to quantitate airway inflammation – vascular and lung parenchymal – as previously described (Starkey et al., 2014). Briefly, the histological scoring on the airways, vascular and parenchymal sites were performed individually and respectively. The inflammatory status of the 3 sites was scored from the least to most severe of inflammation in airways (0–4) and parenchymal (0–5) with the assessor blind to the biological groups. The final scores for airway histology inflammation were the average score for 6 mice per group, with 6 areas of view for each mouse for scoring. The expression of MUC5B in the lungs was detected by immunohistochemical analysis. Briefly, the sections were dewaxed,

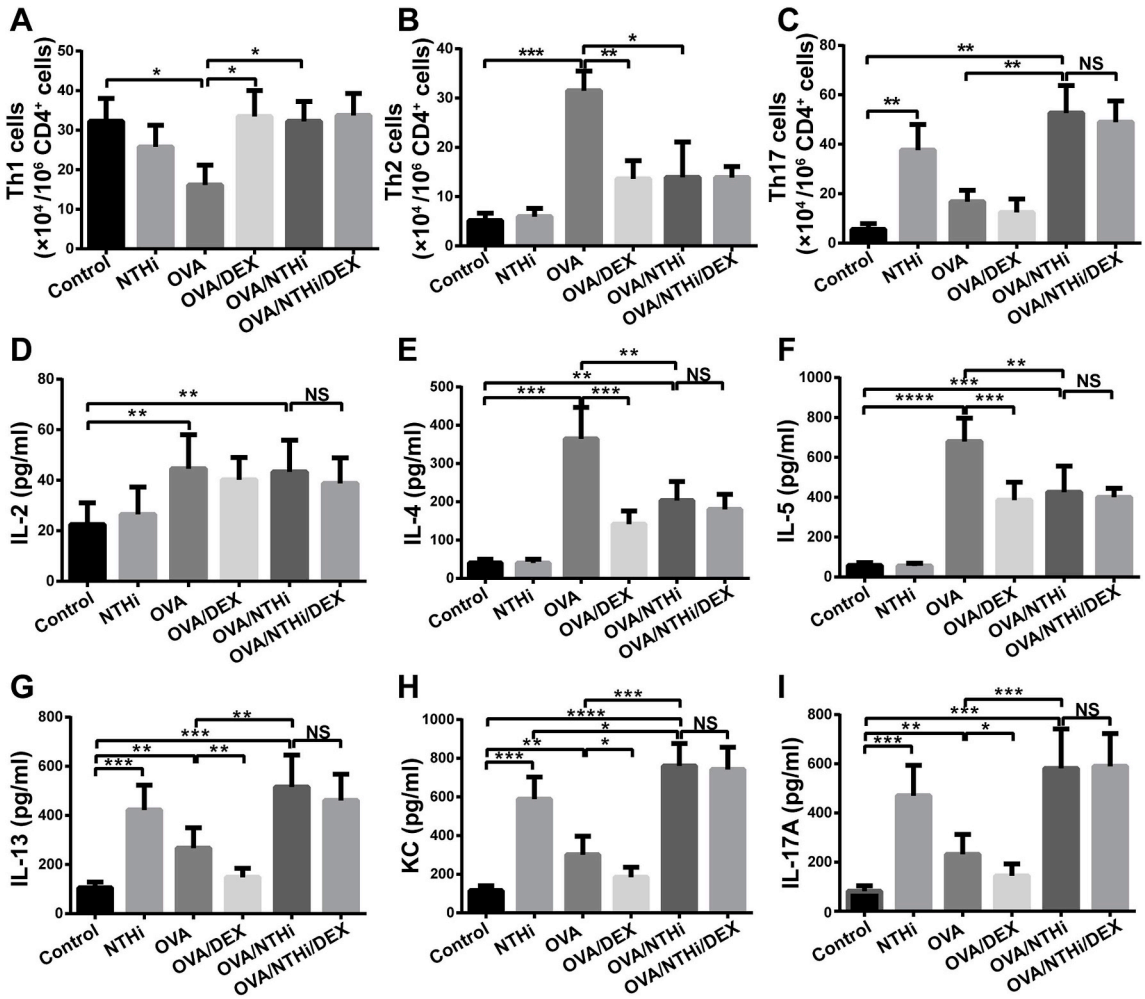


**Fig. 4.** NTHi infection suppresses the Th2 response and enhances the Th17 response in AAD. The numbers of **(A)** Th1 ($CD4^+INF\text{-}\gamma^+$) cells, **(B)** Th2 ($CD4^+IL\text{-}4^+$) cells, and Th17 ($CD4^+IL\text{-}17^+$) cells among $10^6$ $CD4^+$ cells were determined by flow cytometry FCM. The levels of **(D)** IL-2, **(E)** IL-4, **(F)** IL-5, **(G)** IL-13, **(H)** KC, and **(I)** IL-17A were measured by ELISAs. Data are presented as mean ± S.D., n = 6, $^*P < 0.05$; $^{**}P < 0.01$; $^{***}P < 0.001$; $^{****}P < 0.0001$; NS, non-significant.

dehydrated, and incubated with an anti-MUC5B antibody (Abcam, Cambridge, MA, USA). Optical density values were determined and analysed in Motic Images Advanced (v3.2, Motic Asia Corporation, Hong Kong), a higher OD value represented a higher expression level of MUC5B.

### 2.7. Enzyme-linked immunosorbent assays (ELISAs) and a cytometric bead array

ELISA kits were used to quantify MUC5AC and MUC5B protein levels in lung tissue or BAL fluid (CUSABIO, Wuhan, China). Cytokines (IL-2, IL-4, IL-6, TNF-α, and IL-17A) in BAL fluid were quantified with the Cytometric Bead Array Mouse Th1/Th2/Th17 Cytokine Kit (BD Biosciences, San Diego, CA, USA). IL-1β, IL-5, Keratinocyte-derived Cytokine (KC), and IL-13 levels were measured by ELISAs (RayBio, Atlanta, GA, USA). All the measurements were performed in triplicate.

### 2.8. Flow cytometry

Cells in BAL fluid were incubated with a phycoerythrin (PE)-conjugated anti-CD11b antibody (BD Biosciences) and an allophycocyanin (APC)-conjugated anti-Ly6G antibody (BD Biosciences) and were analysed by flow cytometry (NovoCyte, ACEA, San Diego, CA, USA) to detect neutrophils (Li et al., 2017). T helper cell types in the lungs were also analysed by flow cytometry. Briefly, a mouse lung was excised, homogenised, and digested with type I collagenase (Gibco, Life Technologies) to prepare single-cell suspensions. The cells were stimulated with a leukocyte activation cocktail, which contained phorbol 12-myristate 13-acetate (0.1 mg/ml), ionomycin (1 mg/ml), and a protein transport inhibitor (BD GolgiPlug) for 4 h. The cells were resuspended in PBS and incubated for 30 min with an antibody to a surface marker: a peridinin-chlorophyll protein (PerCP)-conjugated anti-CD4 antibody (BD Biosciences). Then, the cells were washed, fixed with Fix/Perm Buffer (BD Pharmingen) for 50 min, and stained with antibodies against intracellular proteins: an APC-conjugated anti-INF-γ antibody, a PE-

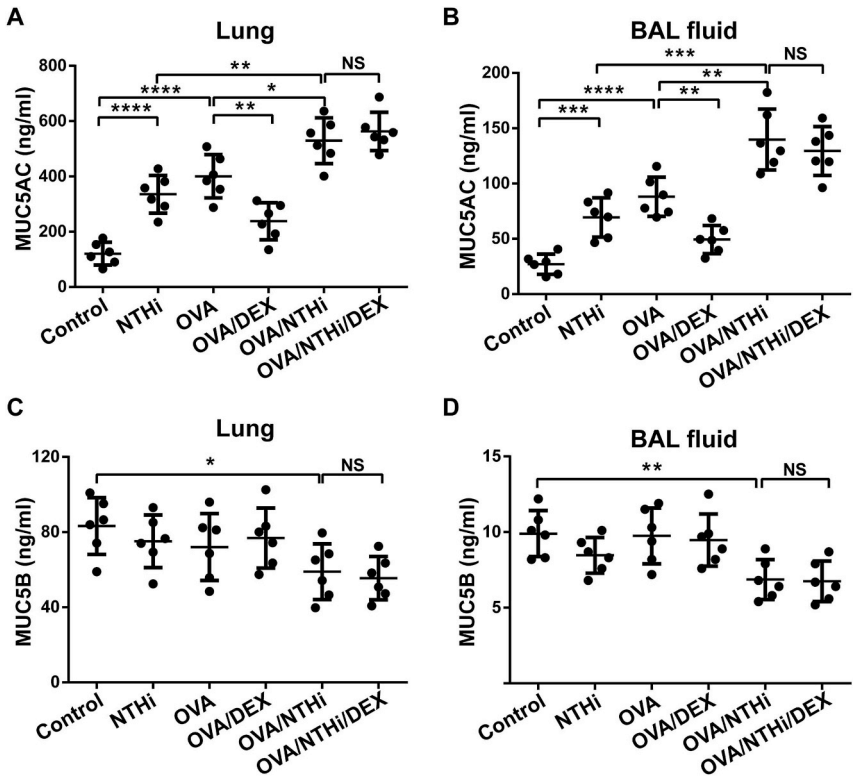


**Fig. 5.** NTHi infection causes higher MUC5AC and lower MUC5B protein levels in AAD. MUC5AC in **(A)** lung homogenates, **(B)** BAL fluid. MUC5B in **(C)** lung homogenates and **(D)** BAL fluid. Data are presented as mean ± S.D., n = 6, $*P < 0.05$; $**P < 0.01$; $***P < 0.001$; $****P < 0.0001$; NS, non-significant.

conjugated anti-IL-4 antibody, and a PE-conjugated anti-IL-17 antibody (BD Biosciences) for 50 min. Finally, the samples were analysed on a flow cytometer, and the data were analysed using FlowJo software (NovoCyte, ACEA).

### 2.9. Western blotting

Mouse lungs were collected, washed, and homogenised in RIPA lysis buffer (Solarbio Technology, Beijing, China) supplemented with a protease inhibitor cocktail and a protein phosphorylation inhibitor (Roche, Indianapolis, IN, USA). The concentrations of total protein were determined via the Enhanced BCA Protein Assay Kit (Beyotime, Jiangsu, China). Total-protein samples (30 μg) were separated by SDS-PAGE in a 12% gel and transferred to polyvinylidene difluoride membranes (Millipore Corp, Billerica, MA, USA). The membranes were blocked with 5% (w/v) non-fat dried milk or BSA for 2 h and incubated with primary antibodies overnight at 4 °C, followed by incubation with a relevant secondary antibody (Sigma-Aldrich) for 1 h at room temperature, and were washed three times in Tris-buffered saline containing 0.1% Tween 20. The signals were detected using the Enhanced Chemiluminescence Kit (Beyotime, Jiangsu, China) and normalised to β-actin data. Antibodies against β-actin (1:10000 dilution), NF-κB p65 (1:2000), and phospho- (p-)p65 (1:2000) as well as a secondary antibody (a horseradish peroxidase-conjugated antibody; 1:10000) (all from Abcam, United Kingdom) were used in the above-mentioned western blots, as were antibodies against p-p38 (1:2000 dilution), total p38 (1:1000), p-p44/42 ERK1/2 (Thr202/Tyr204) (1:2000), ERK1/2 (1:1000), p-p44/42 ERK1/2 (Thr202/Tyr204) (1:2000), and ERK1/2 (1:1000), which were purchased from Cell Signaling Technology (Danvers, MA, USA).

### 2.10. Study protocol approval

This study was carried out in accordance with the principles of the Basel Declaration and recommendations for the handling of laboratory animals (Directive 86/609/EEC in the Protection of Animals Used for Experimental and Other Scientific Purposes, 1986). The protocol was approved by the Institutional Animal Care and Use Committee of Jilin University (permit No. 2017-0034, 13 August 2017).

### 2.11. Statistical analysis

All the analyses were performed in GraphPad Prism (version 6; GraphPad Software, San Diego, CA, USA). The results are presented as mean ± S.D. Comparisons between two groups were conducted with unpaired two-tailed Student's or Welch's *t*-test. Multiple comparisons were performed by One-way analysis of variance (ANOVA) with Tukey-Kramer post hoc analysis. Survival curves were estimated by the Kaplan–Meier method and compared by the log-rank test. Data with $P < 0.05$ were considered significant.

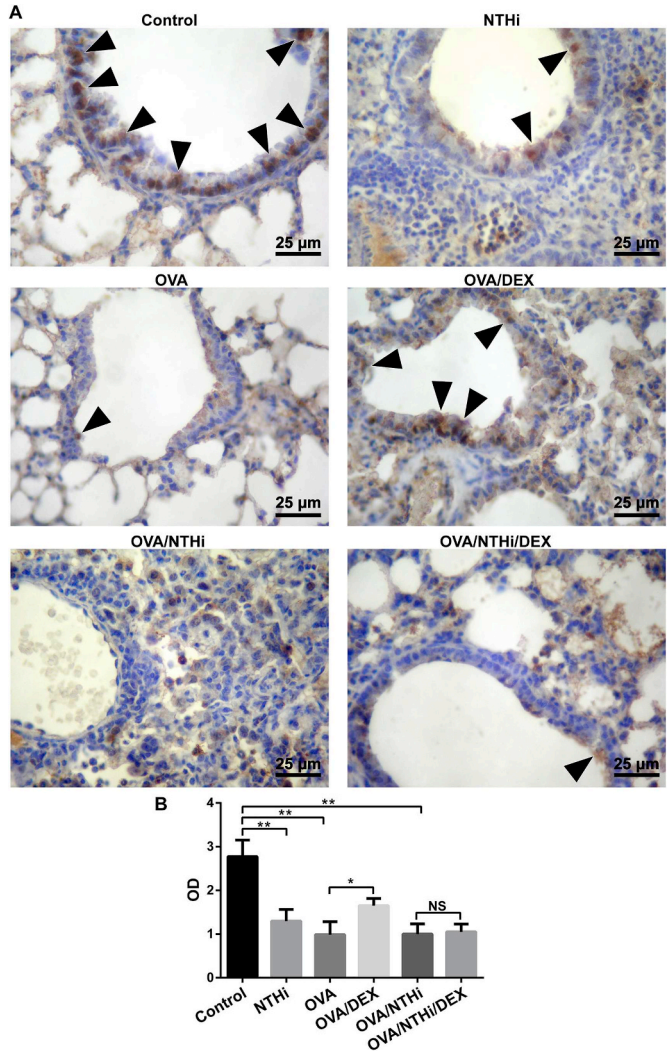


**Fig. 6.** NTHi infection reduced the amount of the MUC5B protein in the lungs. **(A)** The expression of MUC5B (black triangles) in lung sections was detected immunohistochemically. **(B)** Optical density (OD) was measured. Data are presented as mean ± S.D., n = 6, $^{*}P < 0.05$; $^{**}P < 0.01$; NS, non-significant.

## 3. Results

### 3.1. Characterisation of NTHi infection in AAD

To determine whether NTHi infection induces corticosteroid resistance in AAD, we created a murine model of NTHi infection in AAD. The schematic overview of the experimental protocol is presented in Fig. 1A. NTHi-infected AAD mice (the OVA/NTHi group) had significantly higher NTHi loads in the lungs on day 3 post-infection as compared with the group infected with NTHi alone (the NTHi group), the latter mice cleared the majority of NTHi (Fig. 1B). This infection resulted in a significant weight loss in all the mice except for the PBS control group. The OVA/NTHi group manifested a more severe weight loss and a reduced response to dexamethasone therapy (Fig. 1C and D). To assess the effects of NTHi infection on AHR, we examined the respiratory system resistance and lung dynamic compliance in all the groups. Respiratory system resistance was more severe in the OVA group, and this effect was reversed by dexamethasone. Although NTHi infection did not aggravate AHR in comparison with the OVA group, dexamethasone did not reverse AHR in this group (Fig. 1E and F). Similar results were obtained regarding lung dynamic compliance (Fig. 1G and H). These data suggested that NTHi infection is an important cause of steroid resistance.

### 3.2. NTHi infection in AAD aggravates pulmonary neutrophilic inflammation

We assessed pulmonary inflammation by estimating the number of inflammatory cells in BAL fluid. NTHi infection resulted in a significant increase in the total cell counts of neutrophils and lymphocytes as compared with the control group. The OVA group showed a moderate but significant increase in the numbers of total cells, neutrophils and lymphocytes; however, the number of eosinophils was significantly higher as compared with the control and NTHi groups; this phenomenon is a typical clinical feature of allergic asthma. The OVA/NTHi group also showed a significant increase in total cell counts, especially the numbers of neutrophils and lymphocytes, as compared to the NTHi group or OVA group (Fig. 2A–D). Of note, NTHi infection in AAD caused a reduction in eosinophils (Fig. 2C).

To further clarify the involvement of neutrophils, flow cytometry was carried out to identify the proportion of neutrophils in BAL fluid. The results showed that neutrophil numbers were significantly higher in each group than in the control group (Fig. 2E and F). In particular, NTHi infection in AAD significantly increased the proportion of neutrophils (up to 80%). Dexamethasone did not reduce the cellular infiltrates in any groups except for the OVA group. This result confirmed that NTHi infection in AAD resulted in steroid resistance.

The levels of proinflammatory cytokines in BAL fluid were measured next. NTHi infection led to significantly higher levels of TNF-α, IL-1β, and IL-6, and these concentrations were further increased by OVA (Fig. 2G–I). Although dexamethasone reduced the production of these cytokines induced by OVA, the OVA/NTHi group manifested the poorest response to dexamethasone.

Similar results were also obtained in lung tissues after H&E staining. Neutrophil infiltrates were notably present in the airways, blood vessels, and lung parenchyma in the NTHi group and were even greater in the OVA/NTHi group. In the OVA group, numerous infiltrating eosinophils were observed around the airway as compared with the control group. This problem was effectively alleviated by dexamethasone. In contrast, the OVA/NTHi group showed a decreasing trend of eosinophils as compared with the OVA group (Fig. 3A and Fig. S1A). In terms of the histological score, both groups NTHi and OVA/NTHi showed greater histological changes as compared with controls, and these effects were not reversed by dexamethasone (Fig.3B and Fig. S1B).

### 3.3. NTHi infection attenuates the Th2 response and enhances the Th17 response in AAD

We investigated the numbers of Th1 cells (defined as $CD4^{+}INF\text{-}\gamma^{+}$), Th2 cells (defined as $CD4^{+}IL\text{-}4^{+}$), and Th17 cells (defined as $CD4^{+}IL\text{-}17^{+}$) in the lung tissues of each group. NTHi infection led to a Th17 response without affecting the numbers of Th1 and Th2 cells in comparison with the control group. The number of Th2 cells was significantly higher, while that of Th1 cells was markedly lower in the OVA group than in the control group. This unbalanced Th1/Th2 ratio in the OVA group was effectively normalised by dexamethasone

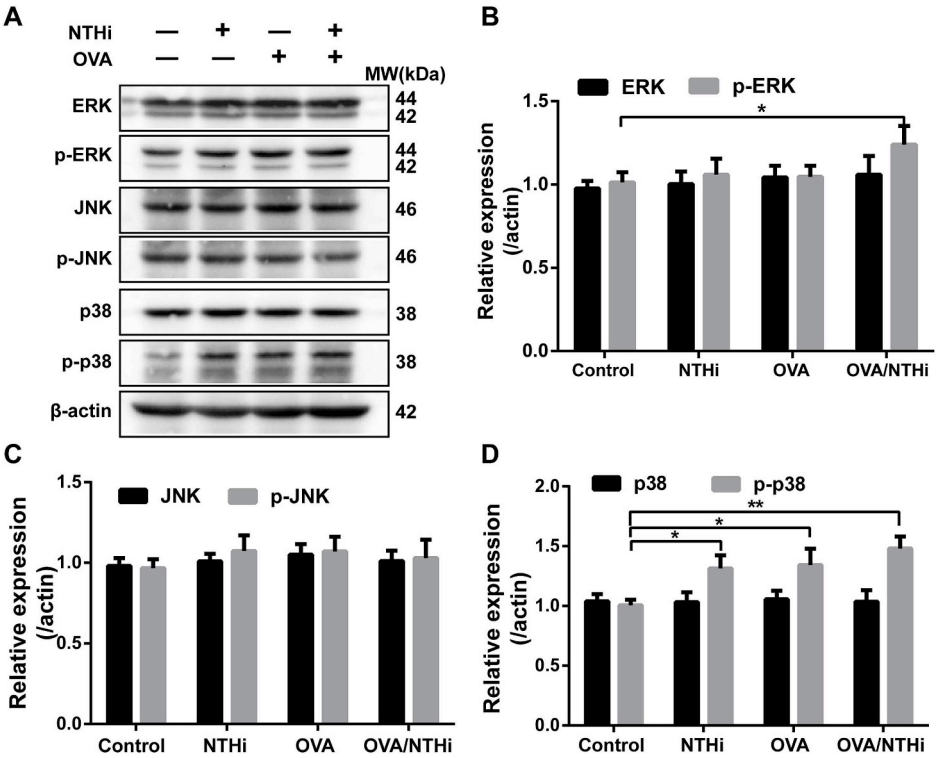


**Fig. 7.** Elevated p38 MAPK activity in NTHi-induced SRAAD. **(A)** Levels of three major MAPK proteins (total and phosphorylated) were determined, and the densitometric values of **(B)** ERK and p-ERK, **(C)** JNK and p-JNK, and **(D)** p38 and p-p38 were calculated. Data are presented as mean ± S.D., n = 6, $^{*}P < 0.05$; $^{**}P < 0.01$; NS, non-significant.

treatment. However, in the OVA/NTHi group, the number of Th2 cells was dramatically lower than that in the OVA group (Fig. 4A and B; Fig. S2A in the online supplement). This finding was consistent with the reduced number of eosinophils in BAL fluid. Of note, the number of Th17 cells was even greater in the OVA/NTHi group compared with the NTHi group. This increase in the number of Th17 cells in the NTHi/OVA group was also resistant to the effects of dexamethasone. There was no significant difference between the OVA and control group (Fig. 4C and S2B).

Furthermore, we measured the levels of Th1 cytokines (IL-2), Th2 cytokines (IL-4, IL-5, and IL-13), and Th17 cytokines (IL-17A) in lung tissues. IL-2 was not induced by NTHi, but its levels were markedly higher in groups OVA and OVA/NTHi (Fig. 4D). The levels of IL-4, IL-5, and IL-13 were substantially higher in the OVA group than in the control group, and these increases were significantly attenuated by dexamethasone. Expression of IL-4 and IL-5 was not altered by NTHi infection relative to the controls but was lower in the OVA/NTHi group than in the OVA group. It is noteworthy that the concentration of IL-13 was much higher in both the NTHi and OVA/NTHi group and was not decreased by dexamethasone (Fig. 4E–G). NTHi infection significantly raised the expression levels of KC and IL-17A (the NTHi group), and these levels were even higher in the OVA/NTHi group but failed to be reduced by dexamethasone. In the OVA group, the levels of KC and IL-17A were also significantly higher relative to the control group and were effectively reduced by dexamethasone (Fig. 4H and I). These data indicated that NTHi infection in AAD attenuated the Th2 cell response and enhanced the Th17 response and responsiveness to dexamethasone.

### 3.4. NTHi infection aggravates mucus hyper-secretion

To determine the effect of NTHi infection on airway mucus hyper-secretion, we examined the expression levels of mucin in BAL fluid and lung tissues. In general, the induction patterns of proteins MUC5AC and 5B were similar among all the experimental conditions, and the induction magnitude appeared to be higher in the lung tissues than in BAL fluid (Fig. 5A–D). In both lung tissues and BAL fluid, MUC5AC expression was significantly higher in the NTHi group and OVA group than in the controls (Fig. 5A and B). Dexamethasone suppressed the levels of MUC5AC only in the OVA group (not in the OVA/NTHi group; Fig. 5A and B). In contrast, MUC5B protein levels were not affected by NTHi infection and by OVA but were significantly reduced by their combination (the OVA/NTHi group). Dexamethasone had no effect on MUC5B expression (Fig. 5C and D). We also measured the expression of MUC5B immunohistochemically and found that this protein was concentrated in the airway epithelium and was less abundant in the parenchyma (Fig. 6A and B).

### 3.5. NTHi infection exaggerates the activity of p38 MAPK in AAD mice

To determine whether NTHi infection induced steroid-resistant asthma via the MAPK signalling pathway, we examined the activity of p38, ERK, and JNK (Fig. 7A). There were no significant differences in ERK and JNK levels, except that the p-ERK quantity was slightly higher in the OVA/NTHi group than in the control group (Fig. 7B). The amounts of p-p38 were significantly higher in the NTHi group, OVA group, and OVA/NTHi group (Fig. 7D). These results indicated that the increased p38 activity could contribute to the pathogenesis of NTHi-induced steroid resistance in AAD.

### 3.6. SB203580 improves lung function in SRAAD

To further assess the participation of p38 in the pathogenesis of

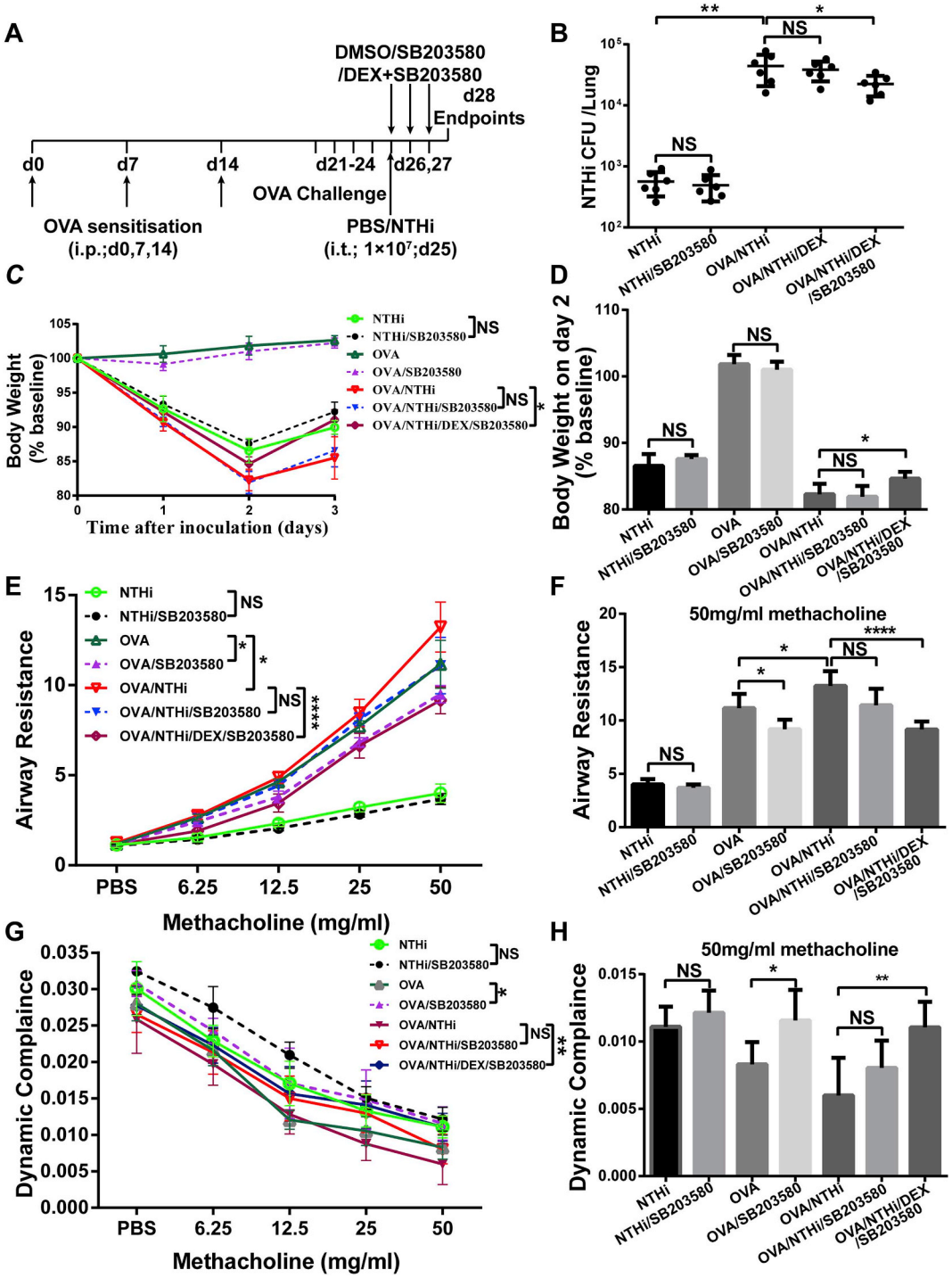


**Fig 8.** p38 MAPK inhibition attenuates the features of NTHi-induced SRAAD. **(A)** The schematic overview of the experimental protocol. BALB/c mice were sensitised i.p. with OVA/alum (on days 0, 7, and 14) and were challenged with the OVA aerosol (on days 21–24). After that, the mice received 30 μl ($10^7$ CFUs) of NTHi (day 25) i.t. to induce SRAAD. The mice were i.p injected (days 25–27) with dexamethasone, SB203580 (5 mg/kg), or DMSO (vehicle) or a combination of dexamethasone and SB203580. All disease parameters were measured on day 28. **(B)** The NTHi load was characterised by bacterial colony counting in the lung homogenates. **(C)** Body weight loss is shown as a percentage of baseline. **(D)** The plot of body weight on day 2 after NTHi infection. **(E)** Respiratory system resistance in response to increasing concentrations of methacholine, **(F)** respiratory system resistance in response to 50 mg/ml methacholine, **(G)** dynamic compliance in response to increasing concentrations of methacholine, and **(H)** dynamic compliance in response to 50 mg/ml methacholine. Data are presented as mean ± S.D., n = 6, $^*P < 0.05$; $^{**}P < 0.01$; $^{***}P < 0.001$; NS, non-significant.

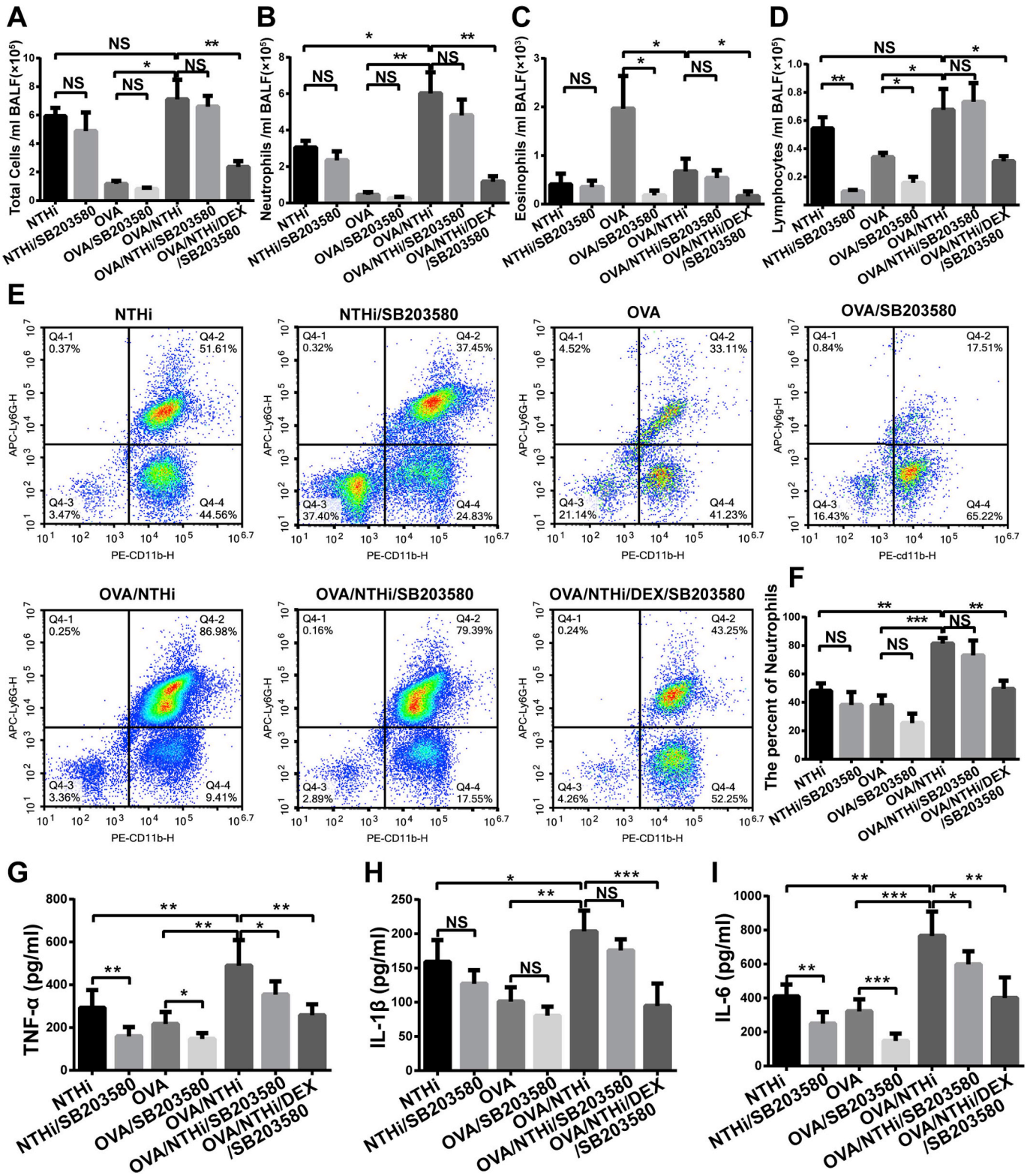


**Fig. 9.** Suppression of signs of NTHi-induced neutrophilic inflammation in BAL fluid by the combination of dexamethasone and SB203580. **(A)** All cells, **(B)** neutrophils, **(C)** eosinophils, and **(D)** lymphocytes were counted in BAL fluid under a microscope. **(E)** Neutrophils in BAL fluid was detected by flow cytometry, and **(F)** the percentage was analysed. **(G)** TNF-α, **(H)** IL-1β, and **(I)** IL-6 in BAL fluid were quantitated by ELISAs. Data are presented as mean ± S.D., n = 6, $^{*}P < 0.05$; $^{**}P < 0.01$; $^{***}P < 0.001$; NS, non-significant.

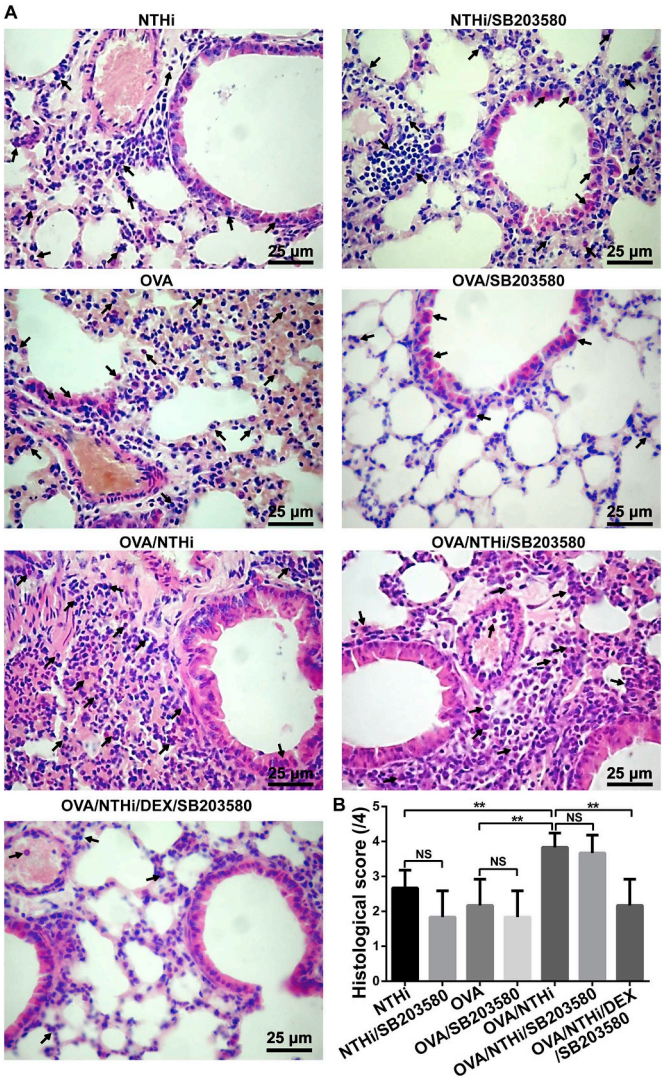


**Fig. 10.** Combined treatment with SB203580 and dexamethasone inhibits pulmonary neutrophilic inflammation in murine lungs. **(A)** Inflammatory infiltrates in the lungs were assessed by H&E staining (black arrowheads indicate inflammatory cells in the lung). **(B)** The histological score was estimated from H &E staining of lung sections. Data are presented as mean ± S.D., n = 6, $^{*}P < 0.05$; $^{**}P < 0.01$; NS, non-significant.

steroid resistance in AAD, a specific pharmacological inhibitor of p38, SB203580, was administered on the same day as NTHi infection and every day after the infection till day 28. The dose response in the SB203580 experiment revealed that daily administration of SB203580 at 5 mg/kg was effective in reducing NTHi-induced mortality (Fig. S3). To evaluate the influence of SB203580 on the steroid resistance, in a parallel experiment, both SB203580 and dexamethasone were administered in combination (Fig. 8A). SB203580 alone significantly improved respiratory system resistance and lung compliance in the OVA group but had little or no effect on NTHi loads in the lungs (Fig. 8B) and failed to improve the weight loss recovery (Fig. 8C and D). The combined administration of SB203580 and dexamethasone mildly attenuated the weight loss and facilitated bacterial clearance from the lungs in the OVA/NTHi group (Fig. 8B–D). Thus, the combined use of SB203580 and dexamethasone protected mice from AHR in the OVA/NTHi group (Fig. 8E–H).

### 3.7. SB203580 potently enhances the efficacy of dexamethasone against inflammation in SRAAD

Next, to test whether SB203580 modulates airway inflammation, inflammatory cells and pro-inflammatory cytokines were quantified in BAL fluid and lung tissues. SB203580 alone had no influence on the total numbers of cells, neutrophils, eosinophils, and lymphocytes in groups NTHi and OVA/NTHi, except for lymphocytes in the NTHi group (Fig. 9A–D). Moreover, in the OVA group, both eosinophil and lymphocyte numbers were effectively reduced by SB203580 alone (Fig. 9C and D). In contrast, SB203580 and dexamethasone co-treatment significantly suppressed the inflammation, e.g. by reducing the number of inflammatory cells and the secretion of inflammatory cytokines into BAL fluid and lung tissue (Figs. 9 and 10 and S4). These data suggested that SB203580 cannot effectively attenuate inflammation in steroid-resistant asthma but enhances the ability of dexamethasone to reduce inflammatory cellular infiltrates.

### 3.8. Combined SB203580 and dexamethasone treatment inhibits the Th17 response in SRAAD

We demonstrated that NTHi infection switched the Th2-dominant response in AAD mice to a Th17 response. To determine whether inhibition of p38 affects this Th2–Th17 switch, we assessed the levels of the Th17 response in SB203580- and/or dexamethasone-treated mice. Interestingly, SB203580 alone had no significant effect on Th1, Th2, or Th17 cells in all the groups (Fig. 11A–C and S5). SB203580 significantly downregulated the Th2 cytokines in the OVA group but reduced only the level of IL-13 in other groups (Fig. 11E–G). In addition, SB203580 alone did not reduce the levels of KC and IL-17A in all the groups (Fig. 11H and I). However, combined SB203580 and dexamethasone treatment not only significantly reduced the number of Th17 cells and the levels of KC and IL-17A in SRAAD mice but also decreased the levels of Th2 cytokines (Fig. 11E–I). Collectively, our results provide strong evidence that co-treatment with SB203580 and dexamethasone does not have a simple additive effect; rather, SB203580 enhances the sensitivity of SRAAD mice to dexamethasone treatment (i.e. the effect is synergistic).

### 3.9. Combined treatment with SB203580 and dexamethasone downregulates MUC5AC and MUC5B in SRAAD

SB203580 treatment alone reduced the expression of MUC5AC in both the OVA and OVA/NTHi group but did not affect MUC5B expression (Figs. 12 and 13). Combined SB203580 and dexamethasone treatment significantly attenuated the abnormal expression of MUC5AC and MUC5B in SRAAD.

### 3.10. SB203580 inhibits the phosphorylation of p38 and of NF-κB

To identify the specific target of SB203580, the phosphorylation of p38 and NF-κB was measured. SB203580 significantly inhibited the phosphorylation of p38 but had no effect on the total level of the p38 protein (Fig. 14A–C). Moreover, the data showed that SB203580 had a certain inhibitory effect on the total amount of NF-κB and its phosphorylation (Fig. 14D and E).

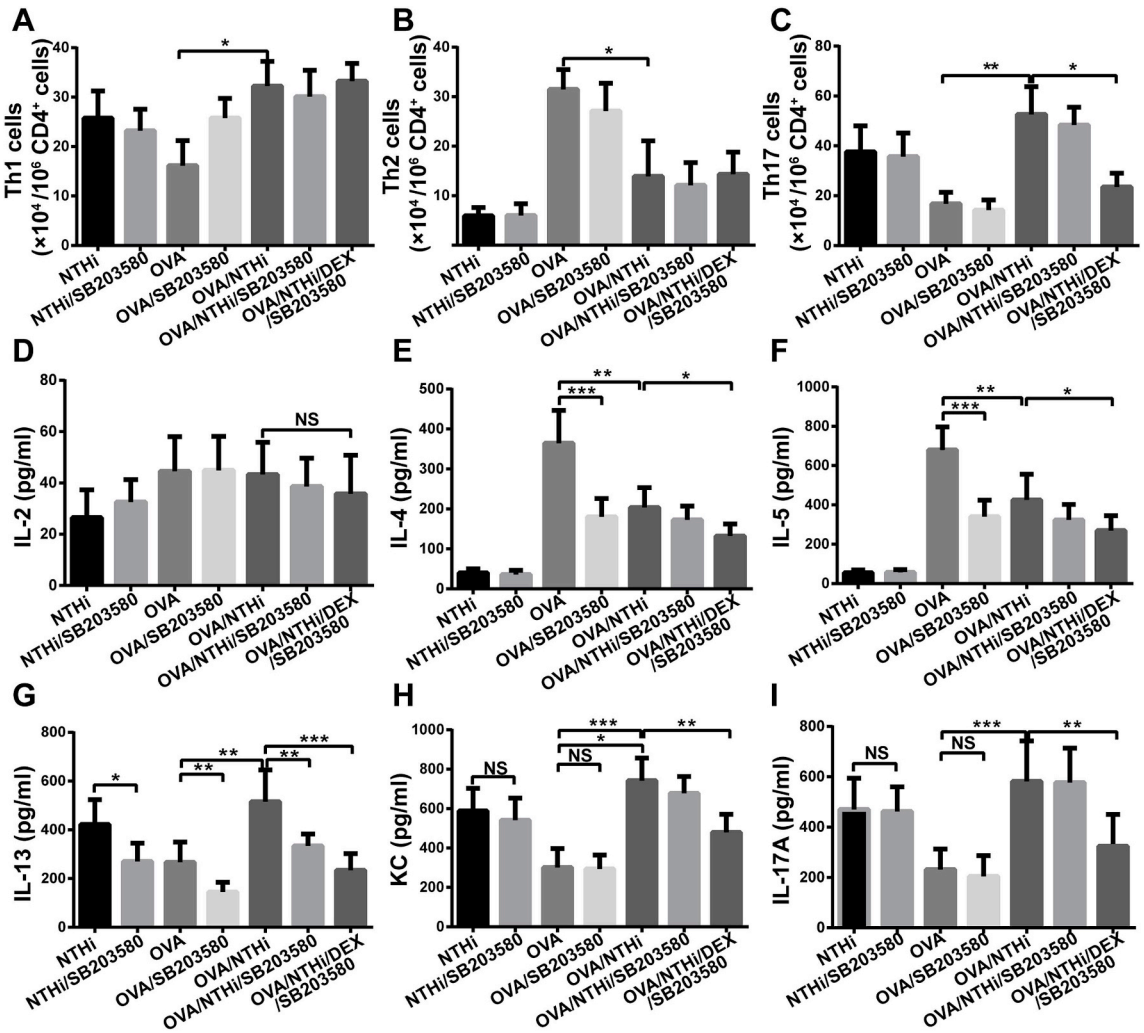


**Fig. 11.** SB203580 only partially downregulated Th2 cytokines, whereas combined SB203580 and dexamethasone treatment significantly inhibited the Th17 response in SRAAD. The numbers of **(A)** Th1 ($CD4^+INF\text{-}\gamma^+$) cells, **(B)** Th2 ($CD4^+IL\text{-}4^+$) cells, and Th17 ($CD4^+IL\text{-}17^+$) cells among $10^6$ $CD4^+$ cells were determined by flow cytometry. The levels of **(D)** IL-2, **(E)** IL-4, **(F)** IL-5, **(G)** IL-13, **(H)** KC, and **(I)** IL-17A were measured by ELISAs. Data are presented as mean ± S.D., n = 6, $*P < 0.05$; $**P < 0.01$; $***P < 0.001$; NS, non-significant.

## 4. Discussion

In this study, we demonstrate that in AAD, NTHi infection aggravates AHR and converts Th2-mediated eosinophilic inflammation into Th17-driven neutrophilic inflammation with increased MUC5AC and MUC5B expression. All these features are poorly responsive to dexamethasone treatment and are consistent with the clinical manifestations of asthma with steroid resistance. We then showed that the increased activity of p38 MAPK is associated with NTHi-induced SRAAD. Interestingly, administration of a specific inhibitor of p38 (SB203580) alone only partially suppressed the prolonged AHR and MUC5AC and MUC5B overexpression and failed to abrogate aggravated neutrophilic inflammation in SRAAD. The combination of SB203580 and dexamethasone effectively reversed these abnormalities, i.e. the immunological features of NTHi-induced SRAAD. This finding indicates that SB203580 may serve as an adjuvant to increase steroid sensitivity and reduce Th17-mediated inflammation in SRAAD.

Similar murine studies have focused on the association between NTHi infection and AAD. However, the impact of NTHi infection on pre-existing AAD has not been assessed. The potential roles of p38 activity in SRAAD have not been demonstrated either. Here, we show that NTHi infection induces prolonged AHR, in agreement with another study (Kim et al., 2017). Contrary to our findings, yet another study revealed that NTHi infection significantly reduces AHR in AAD (Essilfie et al., 2012). This discrepancy may be due to the differences in the NTHi infection period or in other factors such as bacterial strains and assays. In this study, we demonstrate that NTHi infection suppresses OVA-induced Th2 inflammation (including the infiltration of lungs by eosinophils), the levels of Th2 cytokines (IL-4 and IL-5), and the proportion of Th2 cells. Chronic NTHi infection has been reported to inhibit Th2

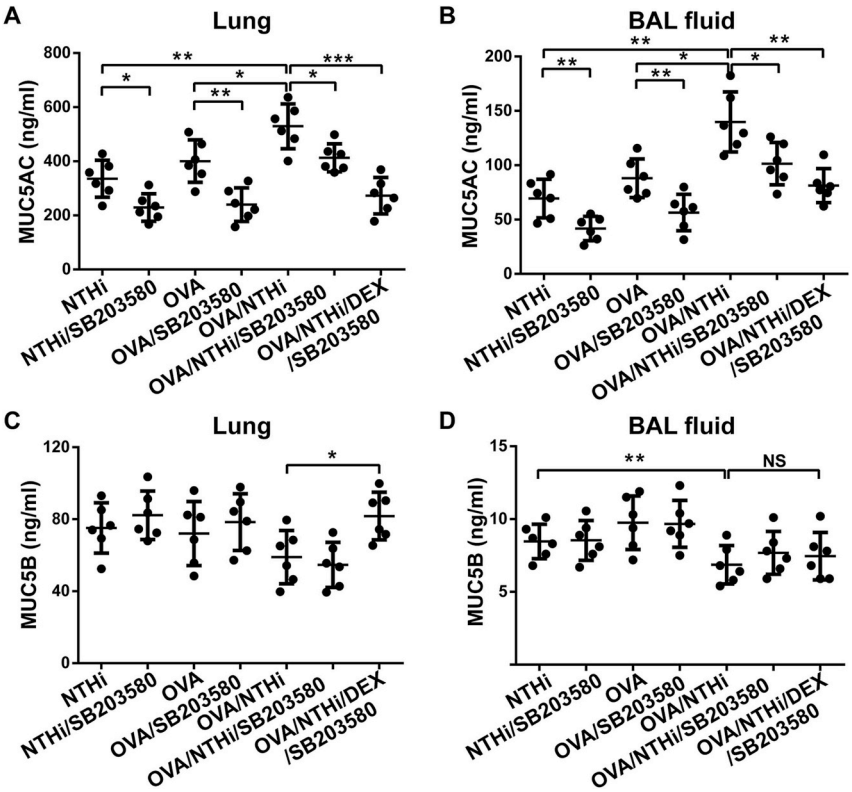


**Fig. 12.** Downregulation of MUC5AC and MUC5B by the combined treatment with SB203580 and dexamethasone in SRAAD. Mucin 5AC (MUC5AC) **(A)** in lung homogenates and **(B)** in BAL fluid. MUC5B **(C)** in lung homogenates and **(D)** in BAL fluid. Data are presented as mean ± S.D., n = 6, $*P < 0.05$; $**P < 0.01$; $***P < 0.001$; NS, non-significant.

responses and to induce a Th17 response in OVA-based models (Essilfie et al., 2012). However, here, we reveal that NTHi infection alone is sufficient to switch the Th2 response to a Th17 response in AAD. It is unknown whether the reduction in the Th2 response is directly caused by the excessive production of IL-17A (Essilfie et al., 2011). Our study also indicates that NTHi induces continuous infiltration of lung tissue by neutrophils, accompanied by high levels of neutrophil chemokines KC and IL-17A. The recruited neutrophils then phagocytose the invading bacteria (Moriyama et al., 2018). Acute inflammatory responses contribute to bacterial clearance, but excessive and chronic inflammation can cause damage to the host.

Mucus hyper-secretion, mucus plugs, and airflow obstruction are important pathological features of fatal asthma (Bonser and Erle, 2017). MUC5AC and MUC5B are the main components of the airway mucus gel. MUC5AC contributes to the pathogenesis of allergen-induced AHR and airway mucus plugging in asthma (Bonser and Erle, 2017). In contrast, MUC5B is critical for airway defence. MUC5B-deficient mice show decreased mucociliary clearance and weaker inflammatory responses (Roy et al., 2014). We showed that NTHi infection upregulated MUC5AC but reduced MUC5B expression in SRAAD. This result is consistent with the clinical study that uncovered a reduction in the MUC5B/5AC ratio in children with acute asthma (Welsh et al., 2017). Dysregulation of gel-forming mucins in asthma is most likely mediated by increased amounts of IL-13, which is known to drive the production of MUC5AC and downregulation of MUC5B in murine models and in human bronchial epithelial cells (Bonser et al., 2016; Evans et al., 2015). Lipopolysaccharide has been found to stimulate the production of IL-13 and promote differentiation into hyper-plastic mucous cells. This observation is consistent with our finding that IL-13 production is increased by NTHi infection (Chand et al., 2018). Moreover, we found that inhibition of p38 MAPK suppressed the expression of IL-13 in all the groups of mice. Similar findings were reported in a study where IL-13-induced MUC5AC expression and mucous-cell metaplasia among mouse tracheal epithelial cells was reversed by a specific inhibitor of p38 (SB202190) (Fujisawa et al., 2008). Furthermore, we showed that NTHi infection significantly increased the weight loss as well as the bacterial load in the lungs of the AAD group. This phenomenon might be associated with decreased capacity for bacterial clearance owing to epithelial tethering of MUC5AC-rich mucus and impaired mucociliary clearance in asthma (Bonser et al., 2016).

Corticosteroids such as dexamethasone are anti-inflammatory agents and are widely used to inhibit the recruitment of inflammatory cells and to downregulate inflammatory cytokines in AAD. Eosinophilic asthma is sensitive to corticosteroids, whereas patients with neutrophilic asthma are corticosteroid resistant, even at higher doses. Here, we found that dexamethasone treatment effectively inhibited OVA-induced AHR, mucus hyper-secretion, and eosinophilic inflammation in AAD. However, the key features of NTHi infection in AAD – including neutrophilic inflammation, Th17-mediated responses, AHR, and mucus hyper-secretion – were all poorly controlled by dexamethasone alone. Moreover, we observed that neutrophil numbers were increased by dexamethasone treatment during NTHi infection in AAD. Although the mechanisms remain to be further explored, our data indicate that NTHi infection induces steroid resistance in AAD mice.

MAPK signal transduction mechanisms are involved in the pathogenesis of steroid-resistant asthma (Hansbro et al., 2017). There are three major MAPK pathways, including ERK1/2, JNK, and p38 MAPKs. In particular, p38 MAPK activity has been shown to be highly

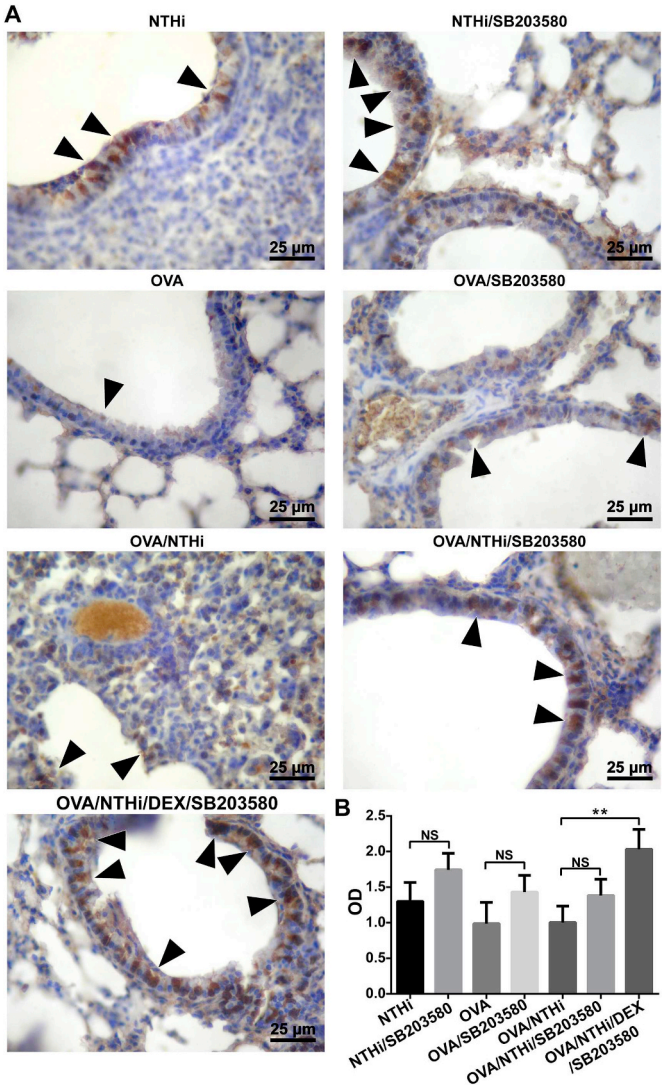


**Fig. 13.** Combined SB203580 and dexamethasone treatment increased the protein expression of MUC5B in the lungs. **(A)** The expression of MUC5B (black triangles) in lung sections was detected immunohistochemically. **(B)** Optical density (OD) was measured. Data are presented as mean ± S.D., n = 6, $^{**}P < 0.01$; NS, non-significant.

correlated with the severity of asthma (Alam and Gorska, 2011). Inhibition of p38 MAPK was reported to reduce corticosteroid insensitivity in patients with severe asthma (Bhavsar et al., 2010). Here, we demonstrated that in AAD, NTHi infection induced phosphorylation of p38 and ERK but not JNK. We also found that SB203580 attenuated eosinophilic airway inflammation, the Th2 response, AHR, and mucus hyper-secretion. These data support the notion that Th2-mediated inflammation can be suppressed by SB203580 (Maneechotesuwan et al., 2007; Tabeling et al., 2017). It is noteworthy that SB203580 treatment only partially suppressed AHR and mucus hyper-secretion in SRAAD mice and had no effect on neutrophilic inflammation. Similar results were obtained in a mouse model of acute lung injury (Chang et al., 2016). However, we cannot rule out the possibility that different doses of SB203580 have different effects on the numbers of neutrophils. Furthermore, a combination of SB203580 and dexamethasone substantially attenuated all the pathological changes induced by NTHi infection in AAD. Given that SB203580 or dexamethasone alone failed to reduce neutrophilic inflammation, the effective inhibition of this feature may not be necessarily due to the additive effect of these two drugs. It was reported that activation of p38 MAPK causes phosphorylation of glucocorticoid receptors and their functional impairment (Irusen et al., 2002). Thus, it is likely that inhibition of p38 restored glucocorticoid receptor function and responsiveness to dexamethasone. We also proved that SB203580 significantly inhibited the phosphorylation of the p65 component of NF-κB, suggesting that SB203580 suppresses neutrophilic inflammation through inhibition of NF-κB activation. However, the exact molecular mechanisms by which SB203580 decreases steroid resistance require further research.

## 5. Conclusions

NTHi infection induced steroid resistance in AAD, promoted the Th2–Th17 switch, exaggerated Th17-mediated neutrophilic inflammation, enhanced AHR, and caused mucus hyper-secretion. These effects were found to be mediated by excessive activation of p38 MAPK. Although inhibition of p38 activity using SB203580 did not effectively attenuate these features, concomitant treatment with dexamethasone significantly ameliorated the key immunological aberrations of SRAAD and Th17-mediated inflammation. Combined treatment with SB203580 and dexamethasone may be a novel therapeutic approach to NTHi-induced SRAAD.

## Funding

The project was funded by Key Laboratory of Health and Family Planning Commission of Jilin Province (Grant no. 3D5172303426), Provincial School Co-construction Industrialization Demonstration Project of Jilin Province (Grant No. SXGJSF2017-1-1(01)) and “the Fundamental Research Funds for the Central Universities”.

## Conflicts of interest

The authors declare that no conflicts of interest.

## CRediT authorship contribution statement

**Guoqiang Wang:** Conceptualization, Methodology, Formal analysis, Writing - original draft. **Zhiqiang Pang:** Methodology, Validation, Formal analysis, Writing - original draft. **Alan Chen-Yu Hsu:** Conceptualization, Writing - review & editing. **Xuewa Guan:** Methodology, Formal analysis, Writing - original draft. **Nan Ran:** Methodology, Data curation. **Yuze Yuan:** Methodology, Data curation. **Ziyan Wang:** Validation. **Yingqiao Guo:** Validation. **Ruipeng Zheng:** Validation. **Fang Wang:** Conceptualization, Writing - review & editing, Supervision, Project administration, Funding acquisition.

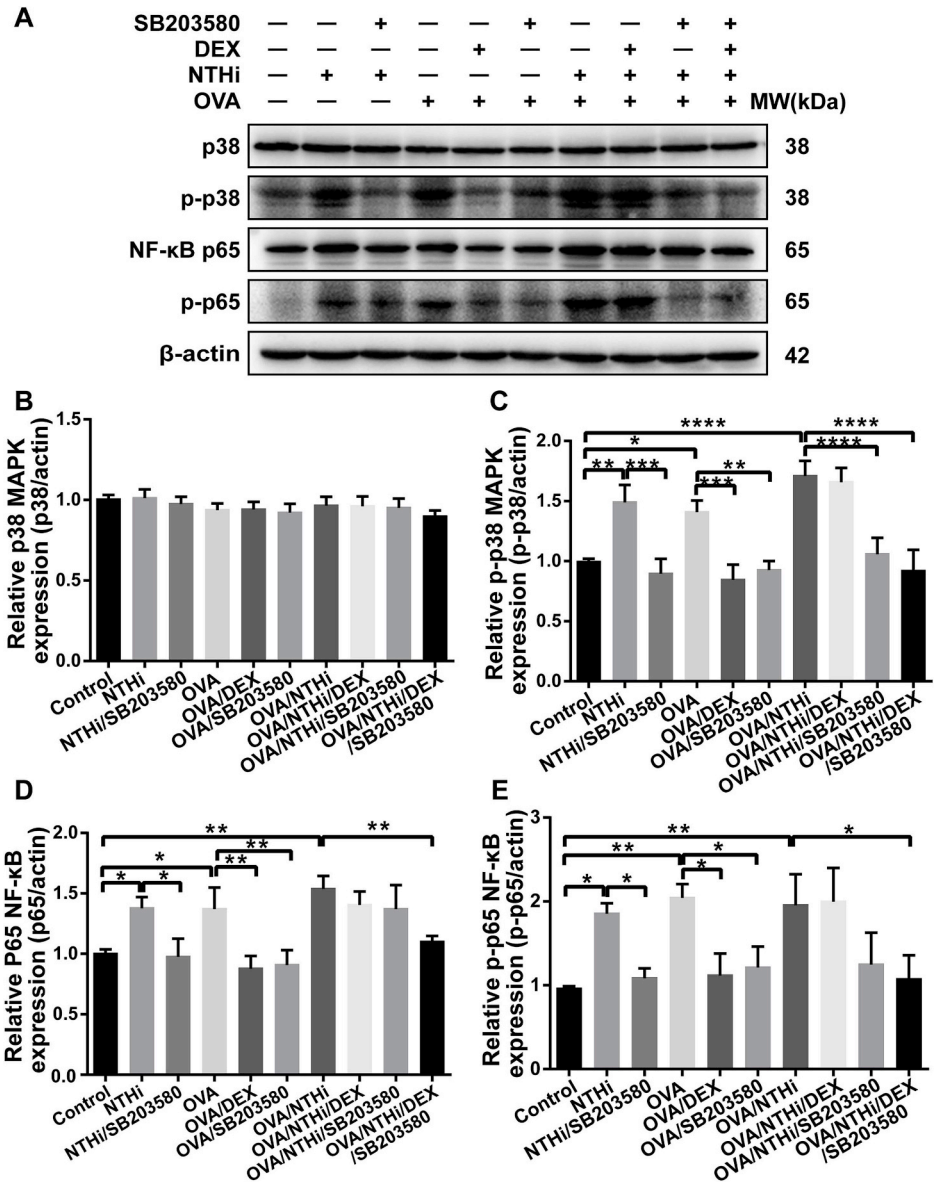


**Fig. 14.** SB203580 suppresses NTHi-induced corticosteroid resistance in allergic airway disease (AAD) through a decrease in the phosphorylation of p38 and of NF-κB. **(A)** Levels of total and phosphorylated p38 mitogen-activated protein kinase (MAPK) and NF-κB p65 were evaluated by western blotting (WB). Optical densities of **(B)** total p38, **(C)** p-p38, **(D)** total p65, and **(E)** p-p65 were measured. Data are presented as mean ± S.D., n = 6, $*P < 0.05$; $**P < 0.01$; $***P < 0.001$; $****P < 0.0001$.

## Appendix A. Supplementary data

Supplementary data to this article can be found online at https://doi.org/10.1016/j.ejphar.2019.172623.

## References

Afshar, R., Strassner, J.P., Seung, E., Causton, B., Cho, J.L., Harris, R.S., Hamilos, D.L., Medoff, B.D., Luster, A.D., 2013. Compartmentalized chemokine-dependent regulatory T-cell inhibition of allergic pulmonary inflammation. J. Allergy Clin. Immunol. 131, 1644–1652.

Alam, R., Gorska, M.M., 2011. Mitogen-activated protein kinase signalling and ERK1/2 bistability in asthma. Clin. Exp. Allergy 41, 149–159.

Bhavsar, P., Hew, M., Khorasani, N., Torrego, A., Barnes, P.J., Adcock, I., Chung, K.F., 2008. Relative corticosteroid insensitivity of alveolar macrophages in severe asthma compared with non-severe asthma. Thorax 63, 784–790.

Bhavsar, P., Khorasani, N., Hew, M., Johnson, M., Chung, K.F., 2010. Effect of p38 MAPK inhibition on corticosteroid suppression of cytokine release in severe asthma. Eur. Respir. J. 35, 750–756.

Bonser, L.R., Erle, D.J., 2017. Airway mucus and asthma: the role of MUC5AC and MUC5B. J. Clin. Med. 6.

Bonser, L.R., Zlock, L., Finkbeiner, W., Erle, D.J., 2016. Epithelial tethering of MUC5AC-rich mucus impairs mucociliary transport in asthma. J. Clin. Investig. 126, 2367–2371.

Chand, H.S., Harris, J.F., Tesfaigzi, Y., 2018. IL-13 in LPS-induced inflammation causes Bcl-2 expression to sustain hyperplastic mucous cells. Sci. Rep. 8, 436.

Chang, S.F., Li, H.C., Huang, Y.P., Tasi, W.J., Chou, Y.Y., Lu, S.C., 2016. SB203580 increases G-CSF production via a stem-loop destabilizing element in the 3' untranslated region in macrophages independently of its effect on p38 MAPK activity. J. Biomed. Sci. 23, 3.

Chung, K.F., 2011. p38 mitogen-activated protein kinase pathways in asthma and COPD. Chest 139, 1470–1479.

Durack, J., Lynch, S.V., Nariya, S., Bhakta, N.R., Beigelman, A., Castro, M., Dyer, A.M., Israel, E., Kraft, M., Martin, R.J., Mauger, D.T., Rosenberg, S.R., Sharp-King, T., White, S.R., Woodruff, P.G., Avila, P.C., Denlinger, L.C., Holguin, F., Lazarus, S.C., Lugogo, N., Moore, W.C., Peters, S.P., Que, L., Smith, L.J., Sorkness, C.A., Wechsler, M.E., Wenzel, S.E., Boushey, H.A., Huang, Y.J., National Heart, L., Blood Institute's, A., 2017. Features of the bronchial bacterial microbiome associated with atopy, asthma, and responsiveness to inhaled corticosteroid treatment. J. Allergy Clin. Immunol. 140, 63–75.

Essilfie, A.T., Simpson, J.L., Dunkley, M.L., Morgan, L.C., Oliver, B.G., Gibson, P.G., Foster, P.S., Hansbro, P.M., 2012. Combined Haemophilus influenzae respiratory infection and allergic airways disease drives chronic infection and features of neutrophilic asthma. Thorax 67, 588–599.

Essilfie, A.T., Simpson, J.L., Horvat, J.C., Preston, J.A., Dunkley, M.L., Foster, P.S., Gibson, P.G., Hansbro, P.M., 2011. Haemophilus influenzae infection drives IL-17-mediated neutrophilic allergic airways disease. PLoS Pathog. 7, e1002244.
Evans, C.M., Raclawska, D.S., Ttofali, F., Liptzin, D.R., Fletcher, A.A., Harper, D.N., McGing, M.A., McElwee, M.M., Williams, O.W., Sanchez, E., Roy, M.G., Kindrachuk, K.N., Wynn, T.A., Eltzschig, H.K., Blackburn, M.R., Tuvim, M.J., Janssen, W.J., Schwartz, D.A., Dickey, B.F., 2015. The polymeric mucin Muc5ac is required for allergic airway hyperreactivity. Nat. Commun. 6, 6281.
Fujisawa, T., Ide, K., Holtzman, M.J., Suda, T., Suzuki, K., Kuroishi, S., Chida, K., Nakamura, H., 2008. Involvement of the p38 MAPK pathway in IL-13-induced mucous cell metaplasia in mouse tracheal epithelial cells. Respirology 13, 191–202.
Goleva, E., Jackson, L.P., Harris, J.K., Robertson, C.E., Sutherland, E.R., Hall, C.F., Good Jr., J.T., Gelfand, E.W., Martin, R.J., Leung, D.Y., 2013. The effects of airway microbiome on corticosteroid responsiveness in asthma. Am. J. Respir. Crit. Care Med. 188, 1193–1201.
Guan, X., Lu, Y., Wang, G., Gibson, P., Chen, F., Fang, K., Wang, Z., Pang, Z., Guo, Y., Lu, J., Yuan, Y., Ran, N., Wang, F., 2018. The role of regulatory T cell in nontypeable Haemophilus influenzae-induced acute exacerbation of chronic obstructive pulmonary disease. Mediat. Inflamm. 2018, 8387150.
Hansbro, P.M., Kim, R.Y., Starkey, M.R., Donovan, C., Dua, K., Mayall, J.R., Liu, G., Hansbro, N.G., Simpson, J.L., Wood, L.G., Hirota, J.A., Knight, D.A., Foster, P.S., Horvat, J.C., 2017. Mechanisms and treatments for severe, steroid-resistant allergic airway disease and asthma. Immunol. Rev. 278, 41–62.
Hsu, A.C., Starkey, M.R., Hanish, I., Parsons, K., Haw, T.J., Howland, L.J., Barr, I., Mahony, J.B., Foster, P.S., Knight, D.A., Wark, P.A., Hansbro, P.M., 2015. Targeting PI3K-p110alpha suppresses influenza virus infection in chronic obstructive pulmonary disease. Am. J. Respir. Crit. Care Med. 191, 1012–1023.
Irusen, E., Matthews, J.G., Takahashi, A., Barnes, P.J., Chung, K.F., Adcock, I.M., 2002. p38 Mitogen-activated protein kinase-induced glucocorticoid receptor phosphorylation reduces its activity: role in steroid-insensitive asthma. J. Allergy Clin. Immunol. 109, 649–657.
Khalaf, R.M., Lea, S.R., Metcalfe, H.J., Singh, D., 2017. Mechanisms of corticosteroid insensitivity in COPD alveolar macrophages exposed to NTHi. Respir. Res. 18, 61.
Kim, R.Y., Pinkerton, J.W., Essilfie, A.T., Robertson, A.A.B., Baines, K.J., Brown, A.C., Mayall, J.R., Ali, M.K., Starkey, M.R., Hansbro, N.G., Hirota, J.A., Wood, L.G., Simpson, J.L., Knight, D.A., Wark, P.A., Gibson, P.G., O'Neill, L.A.J., Cooper, M.A., Horvat, J.C., Hansbro, P.M., 2017. Role for NLRP3 inflammasome-mediated, IL-1beta-dependent responses in severe, steroid-resistant asthma. Am. J. Respir. Crit. Care Med. 196, 283–297.
Konduru, A.S., Matsuyama, S., Lee, B.C., Komatsu, K., Li, J.D., 2017. Curcumin inhibits NTHi-induced MUC5AC mucin overproduction in otitis media via upregulation of MAPK phosphatase MKP-1. Int. J. Inflamm. 2017, 4525309.
Li, J.J., Wang, W., Baines, K.J., Bowden, N.A., Hansbro, P.M., Gibson, P.G., Kumar, R.K., Foster, P.S., Yang, M., 2010. IL-27/IFN-gamma induce MyD88-dependent steroid-resistant airway hyperresponsiveness by inhibiting glucocorticoid signaling in macrophages. J. Immunol. 185, 4401–4409.
Li, K., Zhang, Y., Liang, K.Y., Xu, S., Zhou, X.J., Tan, K., Lin, J., Bai, X.C., Yang, C.L., 2017. Rheb1 deletion in myeloid cells aggravates OVA-induced allergic inflammation in mice. Sci. Rep. 7, 42655.
Maneechotesuwan, K., Xin, Y., Ito, K., Jazrawi, E., Lee, K.Y., Usmani, O.S., Barnes, P.J., Adcock, I.M., 2007. Regulation of Th2 cytokine genes by p38 MAPK-mediated phosphorylation of GATA-3. J. Immunol. 178, 2491–2498.
Marri, P.R., Stern, D.A., Wright, A.L., Billheimer, D., Martinez, F.D., 2013. Asthma-associated differences in microbial composition of induced sputum. J. Allergy Clin. Immunol. 131 346-352 e341-343.
McCann, J.R., Mason, S.N., Auten, R.L., St Geme 3rd, J.W., Seed, P.C., 2016. Early-life intranasal colonization with nontypeable Haemophilus influenzae exacerbates Juvenile airway disease in mice. Infect. Immun. 84, 2022–2030.
Moraes, T.J., Sears, M.R., 2018. Lower respiratory infections in early life are linked to later asthma. Thorax 73, 105–106.
Moriyama, M., Hirano, T., Kawano, T., Kadowaki, Y., Kodama, S., Suzuki, M., 2018. Toll-like receptor 4 plays an important role to enhance bacterial clearance from the nose in synergy with triggering receptor expressed on myeloid cells (TREM)-1 expression on polymorphonuclear neutrophils. Int. J. Pediatr. Otorhinolaryngol. 112, 27–33.
Peters, M.C., Kerr, S., Dunican, E.M., Woodruff, P.G., Fajt, M.L., Levy, B.D., Israel, E., Phillips, B.R., Mauger, D.T., Comhair, S.A., Erzurum, S.C., Johansson, M.W., Jarjour, N.N., Coverstone, A.M., Castro, M., Hastie, A.T., Bleecker, E.R., Wenzel, S.E., Fahy, J.V., National Heart, Lung, Blood Institute Severe Asthma Research Program, 2019. Refractory airway type 2 inflammation in a large subgroup of asthmatic patients treated with inhaled corticosteroids. J. Allergy Clin. Immunol. 143, 104–113 e114.
Reddel, H.K., Bateman, E.D., Becker, A., Boulet, L.P., Cruz, A.A., Drazen, J.M., Haahtela, T., Hurd, S.S., Inoue, H., de Jongste, J.C., Lemanske Jr., R.F., Levy, M.L., O'Byrne, P.M., Paggiaro, P., Pedersen, S.E., Pizzichini, E., Soto-Quiroz, M., Szefler, S.J., Wong, G.W., FitzGerald, J.M., 2015. A summary of the new GINA strategy: a roadmap to asthma control. Eur. Respir. J. 46, 622–639.
Roy, M.G., Livraghi-Butrico, A., Fletcher, A.A., McElwee, M.M., Evans, S.E., Boerner, R.M., Alexander, S.N., Bellinghausen, L.K., Song, A.S., Petrova, Y.M., Tuvim, M.J., Adachi, R., Romo, I., Bordt, A.S., Bowden, M.G., Sisson, J.H., Woodruff, P.G., Thornton, D.J., Rousseau, K., De la Garza, M.M., Moghaddam, S.J., Karmouty-Quintana, H., Blackburn, M.R., Drouin, S.M., Davis, C.W., Terrell, K.A., Grubb, B.R., O'Neal, W.K., Flores, S.C., Cota-Gomez, A., Lozupone, C.A., Donnelly, J.M., Watson, A.M., Hennessy, C.E., Keith, R.C., Yang, I.V., Barthel, L., Henson, P.M., Janssen, W.J., Schwartz, D.A., Boucher, R.C., Dickey, B.F., Evans, C.M., 2014. Muc5b is required for airway defence. Nature 505, 412–416.
Simpson, J.L., Daly, J., Baines, K.J., Yang, I.A., Upham, J.W., Reynolds, P.N., Hodge, S., James, A.L., Hugenholtz, P., Willner, D., Gibson, P.G., 2016. Airway dysbiosis: Haemophilus influenzae and Tropheryma in poorly controlled asthma. Eur. Respir. J. 47, 792–800.
Starkey, M.R., Nguyen, D.H., Essilfie, A.T., Kim, R.Y., Hatchwell, L.M., Collison, A.M., Yagita, H., Foster, P.S., Horvat, J.C., Mattes, J., Hansbro, P.M., 2014. Tumor necrosis factor-related apoptosis-inducing ligand translates neonatal respiratory infection into chronic lung disease. Mucosal Immunol. 7, 478–488.
Tabeling, C., Herbert, J., Hocke, A.C., Lamb, D.J., Wollin, S.L., Erb, K.J., Boiarina, E., Movassagh, H., Scheffel, J., Doehn, J.M., Hippenstiel, S., Maurer, M., Gounni, A.S., Kuebler, W.M., Suttorp, N., Witzenrath, M., 2017. Spleen tyrosine kinase inhibition blocks airway constriction and protects from Th2-induced airway inflammation and remodeling. Allergy 72, 1061–1072.
Takeda, M., Ito, W., Tanabe, M., Ueki, S., Kato, H., Kihara, J., Tanigai, T., Chiba, T., Yamaguchi, K., Kayaba, H., Imai, Y., Okuyama, K., Ohno, I., Sasaki, T., Chihara, J., 2009. Allergic airway hyperresponsiveness, inflammation, and remodeling do not develop in phosphoinositide 3-kinase gamma-deficient mice. J. Allergy Clin. Immunol. 123, 805–812.
Wang, F., He, X.Y., Baines, K.J., Gunawardhana, L.P., Simpson, J.L., Li, F., Gibson, P.G., 2011. Different inflammatory phenotypes in adults and children with acute asthma. Eur. Respir. J. 38, 567–574.
Welsh, K.G., Rousseau, K., Fisher, G., Bonser, L.R., Bradding, P., Brightling, C.E., Thornton, D.J., Gaillard, E.A., 2017. MUC5AC and a glycosylated variant of MUC5B alter mucin composition in children with acute asthma. Chest 152, 771–779.

*Supplementary Materials*

# Combined treatment with SB203580 and Dexamethasone suppresses Non-typeable *Haemophilus influenzae*-induced Th17 inflammation response in murine allergic asthma

Guoqiang Wang[a], Zhiqiang Pang[a], Alan Chen-Yu Hsu[b], Xuewa Guan[a], Nan Ran[a], Yuze Yuan[a], Ziyan Wang[a], Yingqiao Guo[c], Ruipeng Zheng[a, d], and Fang Wang[a*]

[a] *Department of Pathogen Biology, College of Basic Medical Sciences, Jilin University, Changchun 130021, China*

[b] *Priority Research Centre for Asthma and Respiratory Diseases, Hunter Medical Research Institute and the University of Newcastle, NSW 2305, Australia*

[c] *Department of Genetics, College of Basic Medical Sciences, Jilin University, Changchun 130021, China*

[d] *Department of Invasive Technology, First Hospital of Jilin University, Changchun 130021, China*

[*]**Correspondence to:** Department of Pathogen Biology, College of Basic Medical Sciences, Jilin University, Changchun 130021, China.

***E-mail address*:** wf@jlu.edu.cn (F. Wang)

## Online supplement

## Supplementary methods

### Screening of inhibitor doses

Female Balb/c mice, six to eight weeks old, were i.t. inoculated with NTHi ($6\times10^5$ colony forming units [CFU], in 30 μl saline) or sterile saline under pentobarbital anesthesia. Then, mice were administered i.p. with 5mg/kg SB203580 one day or three days to screen the optimal dosage of SB203580. Mouse mortality was recorded every 4 hours until 72 hours.

## Supplementary Figures

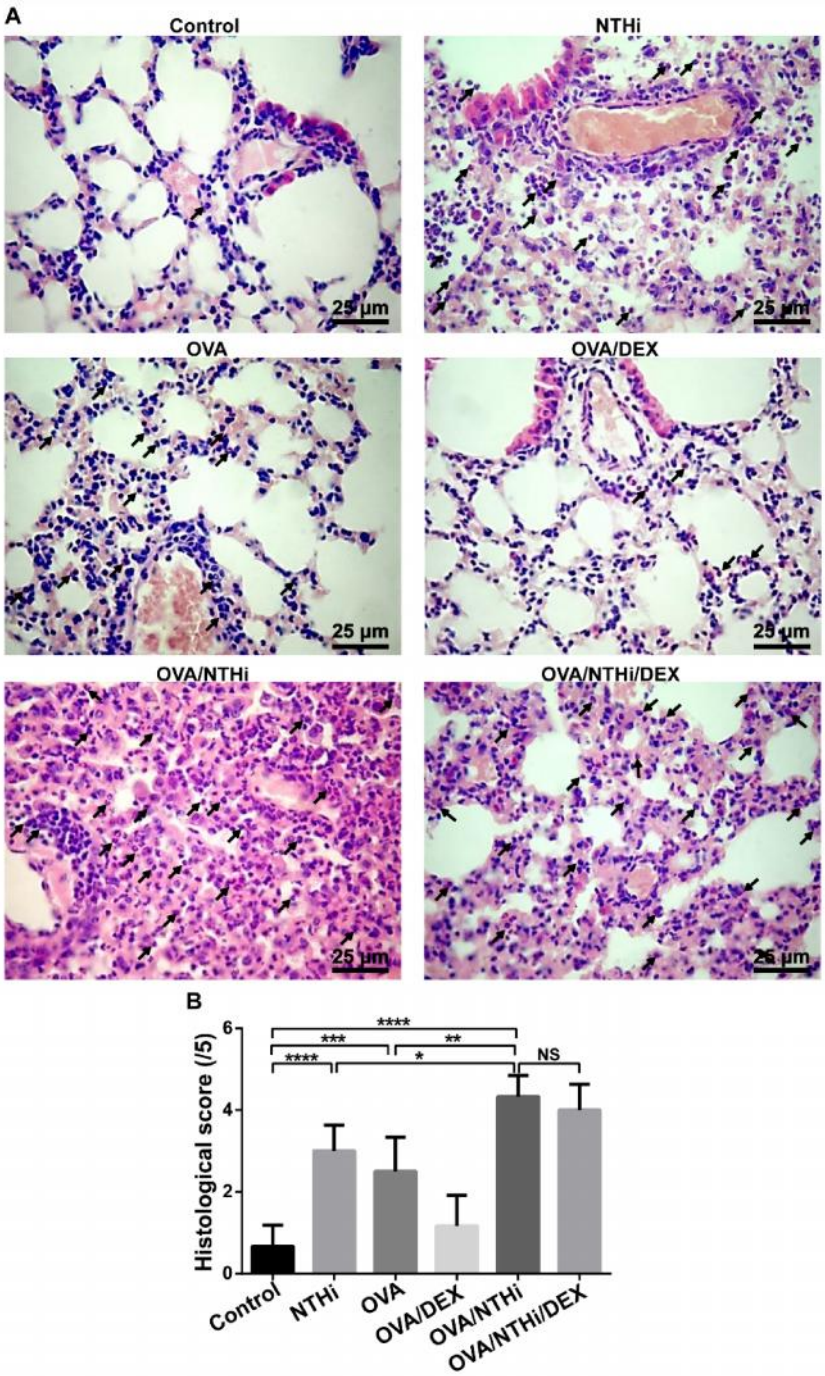


**Fig.S1** NTHi infection aggravates pulmonary neutrophilic inflammation in AAD. **(A)** Inflammatory infiltrates in lungs were determined by H&E staining (black arrowheads indicate inflammatory cells in the lung). **(B)** The histological score was estimated by H&E staining of lung sections. Data are presented as mean ± S.D., n = 6, **P* < 0.05; ***P* < 0.01; ****P* < 0.001; *****P* < 0.0001; NS, non-significant.

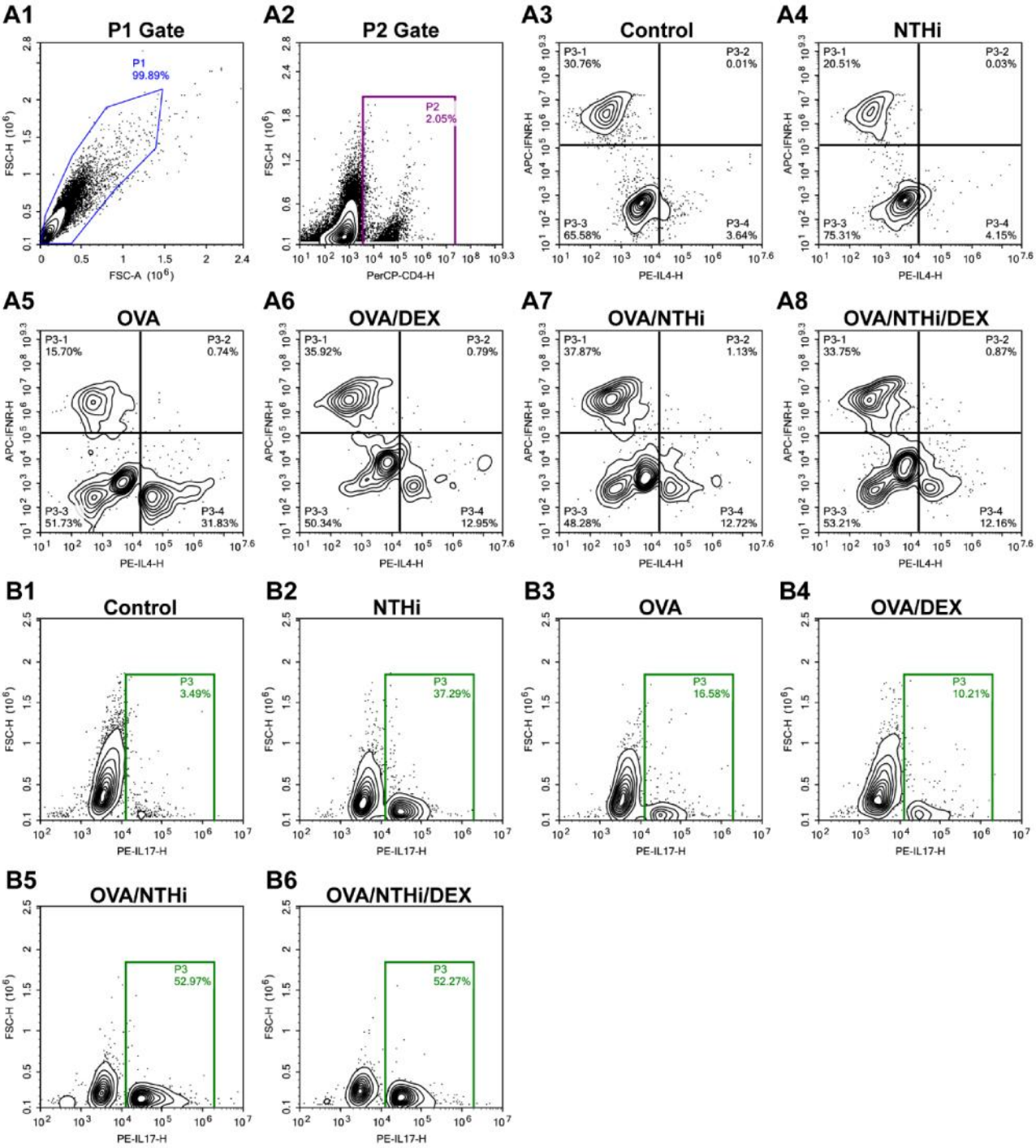


**Fig.S2** NTHi infection decreased Th2 cells and increased Th17 cells in the lungs of AAD mice. **(A1-2)** The P1 and P2 gate. **(A3-8)** The percentage of Th1 ($CD4^{+}INF\text{-}\gamma^{+}$), Th2 ($CD4^{+}IL\text{-}4^{+}$). **(B1-6)** Th17 ($CD4^{+}IL\text{-}17^{+}$) lymphocytes in the lungs of each group were performed through Flow Cytometry. n=6.

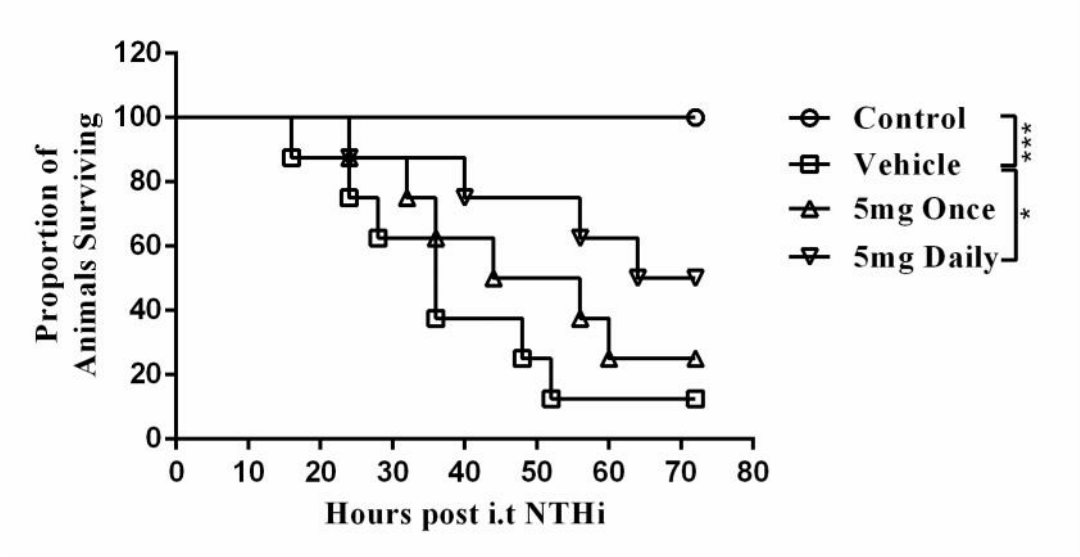


**Fig.S3** Using SB203580 daily can significantly reduce NTHi infection-induced mortality of mice.

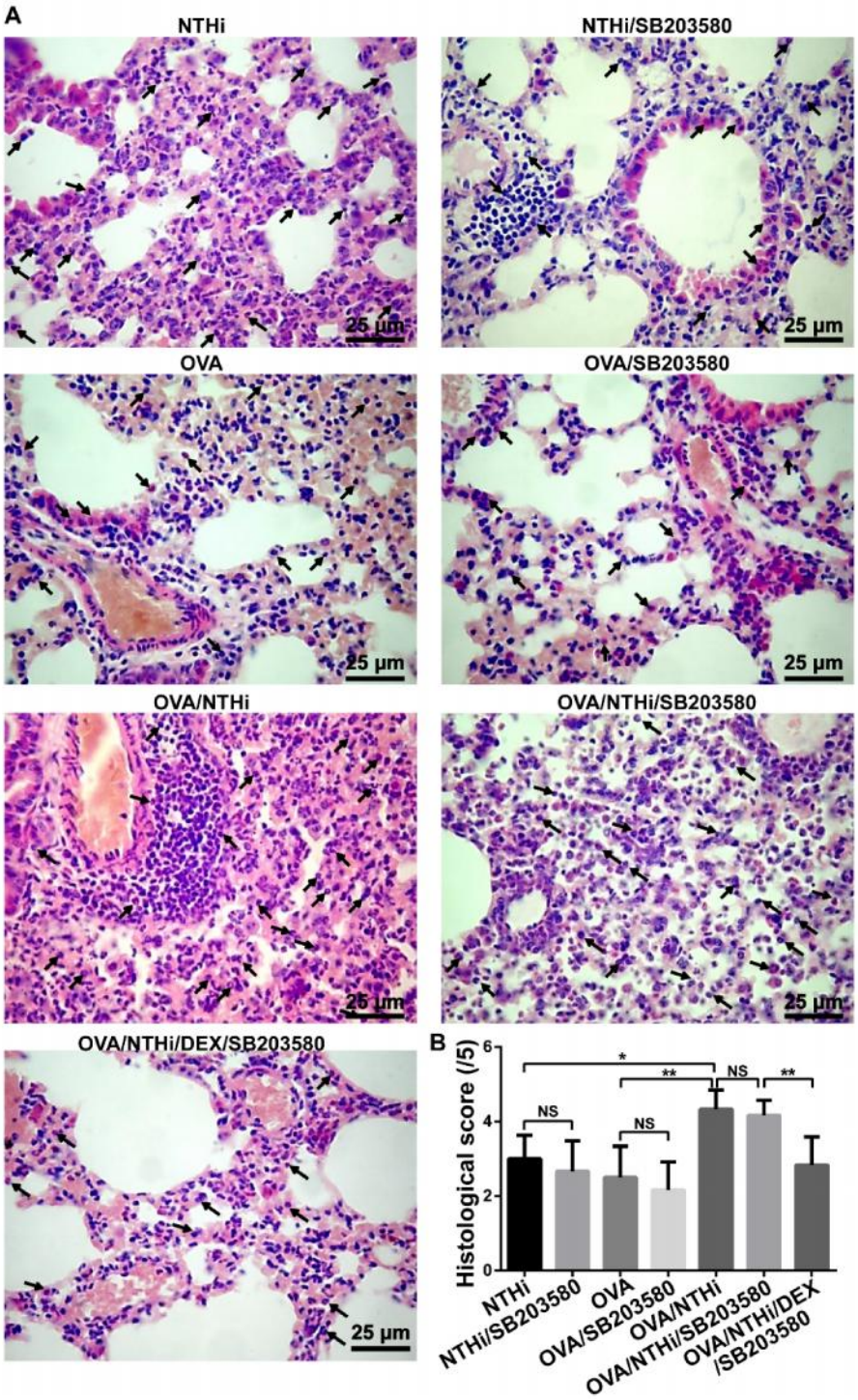


**Fig.S4** Combined treatment with SB203580 and dexamethasone inhibits pulmonary neutrophilic inflammation in murine lungs. **(A)** Inflammatory infiltrates in the lungs were assessed by H&E staining (black arrowheads indicate inflammatory cells in the lung). **(B)** The histological score was estimated from H&E staining of lung sections. Data are presented as mean ± S.D., n = 6, **P* < 0.05; ***P* < 0.01; NS, non-significant.

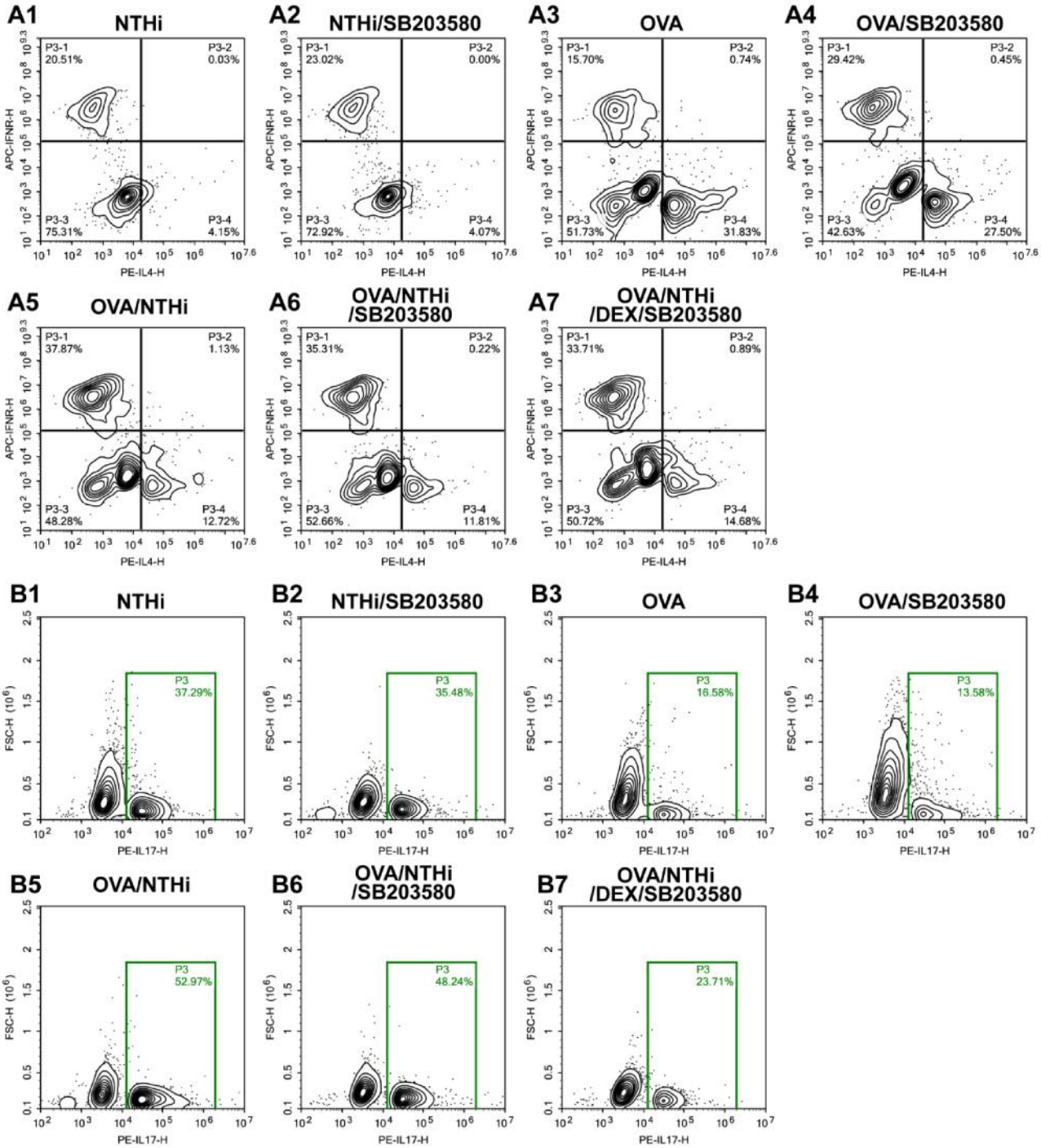


**Fig.S5** Combined SB203580 and dexamethasone treatment significantly reduced Th17 cells in the lungs of SRAAD mice. **(A1-6)** The percentage of TH1 ($CD4^+INF\text{-}\gamma^+$), Th2 ($CD4^+IL\text{-}4^+$). **(B1-6)** Th17 ($CD4^+IL\text{-}17^+$) lymphocytes in the lungs of each group were performed through Flow Cytometry (FCM). n=6.